CHARLES UNIVERSITY

Faculty of Pharmacy in Hradec Králové

Department of Analytical Chemistry

A high-temperature LC-MS method for bottom-up proteomic analyses with reduced artifacts

Mykyta Starovoit

Diploma Thesis

Supervisor: PharmDr. Juraj Lenčo, Ph.D.

Hradec Králové, 2024

I declare that this thesis is my original copyrighted work. All literature and other sources that I have used for elaboration of this thesis are listed in the references and properly cited in the text. The thesis was not used to obtain the same or other academic degree.

Prohlašuji, že tato práce je mým původním autorským dílem. Veškerá literatura a další zdroje, z nichž jsem při zpracování čerpal, jsou uvedeny v seznamu použité literatury a v textu jsou řádně citovány. Práce nebyla použita k získání stejného nebo jiného titulu.

Hradec Králové, 2024 .....

ACKNOWLEDGEMENTS

I would like to kindly acknowledge the efforts of Dr. Lenčo in ensuring the smooth course of this study and giving me insight into the principles of actual scientific workflow. This work would not have resulted in such a quantity of worthy outcomes without Dr. Lenčo's helpfulness and permanent availability for consultations. I would also like to thank the entire research group of Dr. Lenčo for their support in resolving the technical issues that arose during the elaboration of this thesis.

This study was supported by the project of the Czech Science Foundation (GAČR No. 22-21620S).

ABSTRACT

Charles University, Faculty of Pharmacy

Department of Analytical Chemistry

Candidate: Mykyta Starovoit

Supervisor: PharmDr. Juraj Lenčo, Ph.D.

Title of diploma thesis: **A high-temperature LC-MS method for bottom-up proteomic analyses with reduced artifacts**

Proteomic bottom-up LC-MS analyses need more efficient chromatographic separation to keep up with the advances in mass spectrometry and fully exploit the potential of state-of-the-art MS instruments. Elevation of column temperature represents one of the most powerful and cost-effective means for improvement of separation performance. However, high temperature also promotes in-column modification of peptides, putting a spoke in the wheel of sophisticated proteomic analyses.

The current method aims to minimize the formation of temperature-related artifacts via a novel high-flow trap-elute setup with differential column heating. The trap-elute setup reduces the time peptides spend in the heated separation column, resulting in fewer generated artifacts. This mitigates an important drawback of the high column temperature. At the same time, it does not diminish its positive effect on the separation performance. Consequently, the utilization of the elevated column temperature becomes more profitable.

The proposed method reduced the artifact abundance among identified peptides in an exploratory single-shot analysis of a human cell line proteome. It also maintained the number of identified unique peptide sequences comparable to the direct injection configuration. The trap-elute setup was also successfully integrated into a mimicked multi-attribute method for the characterization of therapeutic proteins, where it again reduced analysis-related modification in structure regions with a critical influence on product quality.

Keywords: bottom-up proteomics, liquid chromatography, mass spectrometry, high temperature, artifacts, biopharmaceuticals.

ABSTRAKT

Univerzita Karlova, Farmaceutická fakulta v Hradci Králové

Katedra analytické chemie

Kandidát: Mykyta Starovoit

Školitel: PharmDr. Juraj Lenčo, Ph.D.

Název diplomové práce: **Vysokoteplotní LC-MS metoda pro bottom-up proteomické analýzy se sníženým výskytem artefaktů**

Proteomické bottom-up LC-MS analýzy vyžadují účinnější chromatografickou separaci, aby udržely krok s rozvojem hmotnostní spektrometrie a plně tak využily potenciál i těch nejmodernějších MS přístrojů. Zvýšení teploty separační kolony představuje jedno z nejefektivnějších a nejdostupnějších řešení, jak separaci peptidů v proteomických aplikacích zlepšit. Vysoká teplota však zároveň vede ke vzniku nežádoucích modifikací v chemické struktuře peptidů, což proteomické analýzy významně komplikuje.

Tato metoda je zaměřená na snížení výskytu artefaktů vznikajících na koloně za vysoké teploty. Řešením je zavedení nového vysokoprůtokového *trap-elute* systému za použití rozdílného vyhřívání kolon. Vyvinuté trap-elute uspořádání zkracuje čas, který peptidy stráví na vyhřívané separační koloně, což snižuje počet vzniklých modifikovaných peptidů. Zmirňuje to jeden z negativních následků využití zvýšené teploty, avšak neomezuje její pozitivní vliv na separační účinnost. Ve výsledku se použití vysoké teploty kolony stává výhodnější cestou ke zlepšení separace.

Vyvinutá metoda snížila četnost artefaktů ve vyhledávácí jednonástřikové analýze proteomu lidské buněčné linie a zároveň poskytla počet identifikovaných unikátních peptidových sekvencí srovnatelný s metodou přímého nástřiku. Navrhované uspořádání bylo také úspěšně zavedeno pro charakterizaci terapeutických proteinů, kde opět přispělo k zamezení tvorby nežádoucích modifikací v oblastech s kritickým vlivem na kvalitu léčiva.

Klíčová slova: bottom-up, proteomika, kapalinová chromatografie, hmotnostní spektrometrie, vysoká teplota, artefakty, biofarmaceutika.

TABLE OF CONTENTS

ABBREVIATIONS

AGC	automatic gain control
BEH	Ethylene Bridged Hybrid
CQA	critical quality attribute
CSH	Charged Surface Hybrid
DDA	data-dependent acquisition
DIA	data-independent acquisition
ESI	electrospray ionization
FDR	false discovery rate
HCD	higher-energy collisional dissociation (C-trap dissociation)
HESI	heated electrospray ionization
i.d.	inner diameter
iRT	indexed retention time
MAM	multi-attribute method
PEG	polyethylene glycol
PSM	peptide-spectrum match
PTM	post-translational modification
TCEP	tris(2-carboxyethyl)phosphine hydrochloride
TFA	trifluoroacetic acid
TopN	highest number of the most intense precursor ions selected for fragmentation

1. INTRODUCTION

Bottom-up proteomics based on protein cleavage using a sequence-specific protease followed by analysis utilizing LC-MS has become a core approach in the field [1]. Undoubtedly, the most recent advances here were driven by the progress in mass spectrometry, particularly in data acquisition strategies and data evaluation methods. However, the potential of current state-of-the-art MS instruments cannot be maximally exploited if peptides entering the ion source are not efficiently separated [2]. Elevation of column temperature represents one of the most powerful and accessible solutions for the improvement of separation performance [3]. Nevertheless, besides its positive effect on peak capacity [4]–[6], elevated column temperature also brings a risk of unwanted in-column modification of peptides. Such temperature-related artifacts increase spectra complexity, reduce the concentration of a parent peptide, and compete with them for sequencing while not providing additional relevant biological data. Consequently, artifact formation may overbalance the positive effects of elevated column temperature, eventually resulting in fewer identified peptides. Furthermore, a specific subset of artifacts can hamper the characterization of some post-translational modifications [7][8]. In the case of biopharmaceuticals, it may compromise the accurate quantification of modifications formed during production and storage [9].

In this study, we sought to develop a high-temperature LC-MS method for bottom-up proteomic analyses, which preserves the advantages of elevated column temperature while minimizing in-column peptide modification. The method relies on a trap column installed upstream of the separation column. It has lower retentivity than the separation column and is maintained at a safe temperature. The trap column shortens the residence time of peptides in the heated separation column, leading to reduced modification extent, whereas the separation performance is still preserved. Thus, the concept involves a trap-elute setup that is traditional for nanoLC [10][11]. It is realized in the vented column configuration [12] but has no diversion of the mobile phase from the trap column to waste. The configuration utilizes differential column heating and is developed for the high-flow regime [13]. The method exploits the features of conventional- and microflow separation columns maintained at the highest reasonable temperature of 80 °C [14].

The study begins with selection of the trap column that does not worsen the peak shape of peptides. To approach the best peak shape for both column inner diameters (i.d.), we also examined the effect of the concentration of a mobile phase acidifier and the contribution of the capillary that connects the trap and separation column. Next, to prove the effectivity of the concept, we performed a pilot LC-MS analysis of a bacterial proteome with prepended in-column incubation that simulated a long gradient run. Then, the study proceeded to a test application in an analysis of a human cell line proteome, which mirrors trendy analytical workflows in exploratory proteomics [15], but with an emphasis on analysis-related artifacts. To extend the spectrum of the concept applicability, it was also implemented in a mimicked multi-attribute method (MAM) [16] for the characterization of therapeutic proteins as a way to mitigate the complications originating from utilization of elevated column temperature.

2. AIM OF THE STUDY

The study aims to develop an LC-MS method for bottom-up proteomic analyses that would profit from the advantages of high column temperature while not suffering from extensive artifact formation. The method exploits the trap-elute setup instead of the direct injection configuration that dominates in high-flow LC. Therefore, the most demanding section in the method development is the thorough optimization of the column pair and the analytical conditions to be applied for this setup utilization. The key characteristic of the developed method, which will determine its profitability in comparison to conventional methods, is sensitivity. This is a critical aspect of the use of narrow- and microbore columns [11][17][18]. Therefore, the method providing even worse sensitivity resulting from peak broadening than that typical for high-flow direct injection LC-MS setups would be out of great interest. This is why the principal aim of the study is to reach the separation performance and sensitivity of direct injection on the same separation columns kept at the same temperature.

The more attention-grabbing feature of the method is how effectively it prevents peptides from being modified. First, it depends on the temperature that the peptides are exposed to while being retained in the trap column. Therefore, the aim is to keep the trap column temperature as safe as possible. Also, the modification extent is given by the time that peptides spend in the heated separation column [3]. Hence, it is necessary to select the trap column retentivity as close as possible to the retentivity of the separation column so that peptides spend in the trap column the maximum portion of the total in-column residence time instead of being retained in the heated separation column. However, it comes to a compromise with the need to preserve effective refocusing at the head of the separation column, which is necessary for subsequent efficient separation [10][11]. The underlying condition is to keep sufficient difference between the column retentivities, so the trade-off is to be found.

The following list summarizes the intermediate aims of the study:

1. Selection of trap columns suitable for coupling with the Acquity Premier CSH C_{18} separation columns of 2.1 and 1.0 mm i.d., with emphasis on in-column residence time and the effect of trap column installation on the peak shape; optimization of the trap column temperature; selection of the concentration of the mobile phase acidifier that provides a superior peak shape; selection of the capillary connecting the trap and separation column

3. Proof of the hypothesis that the shortening of in-column residence time due to the trap column installation can reduce the abundance of modified peptides – via an LC-MS analysis of a whole-cell proteome using the trap-elute setup and the direct injection configuration

4. Application of the trap-elute setup in a typical exploratory LC-MS analysis for a comprehensive examination of the impact on method sensitivity, productivity, and modification extent

5. Application of the trap-elute setup in an MAM for orthogonal method assessment and extension of applicability spectrum

3. THEORETICAL SECTION

3.1. Peptides

Peptides are linear polymers of amino acids. There are 22 L-amino acids found *in vivo* as structural units of peptides and proteins; these amino acids are also referred to as biogenic. In proteomics, peptides are mainly considered fragments of proteins since most analyses involve protein cleavage as a source of peptides for further investigation [19][20]. The general definition states that the length of a peptide is 2 to 100 amino acids. As most peptides in a proteomic laboratory are generated by enzymatic cleavage, the peptide length varies depending on the specificity of the used enzyme. For instance, tryptic digestion generates peptides with an average length of 14 amino acids [21]. Besides the number of monomers, the physicochemical properties of peptides are defined by the content of individual amino acids and their positions in sequence. The part of an amino acid with the main impact on peptide properties is a side chain. Side chains of amino acids differ in the length of the hydrocarbon chain, hydrophobicity, and presence of chargeable groups. The latter then defines the acid-base and chelating properties of peptides.

The most noticeable difference between peptides and small-size molecules is in molecular weight and hydrodynamic diameter. While most active pharmaceutical compounds of non-polymeric structure have a molecular weight that does not exceed 1000 Da, the peptide weight can reach several kDa. The larger the molecule, the more active sites for interaction it possesses. This is why large molecules demonstrate high sensitivity to the changes in the mobile phase composition when analyzed with reversed-phase LC [22]. This feature can be described via parameter S, derived from the linear-solvent-strength model of gradient elution introduced by Snyder [23]. The higher the parameter S, the smaller the range of the strong solvent fraction that provides the analyte velocity along the separation column significantly higher than zero but not as high as the mobile phase velocity. As parameter S correlates with molecular weight, the highest values are related to intact proteins. For such large molecules, the retention mechanism likely changes from partitioning between the mobile and stationary phase to adsorption upon injection on the column and desorption at the time when the portion of the strong solvent in the mobile phase approaches a certain value [24]. This process is sometimes simplified as the “catch and release” or “on-off” process [25].

The following consequence of large molecule size is low diffusion rate. Slow diffusion prevents peptides from a quick transfer in and out of the internal pore volume. It leads to worsened mass transfer along the column, which manifests as broadened chromatographic peaks. Although slow diffusion also decreases longitudinal dispersion, leading to peak broadening as well, if these two effects are summed, the negative effect of resistance to mass transfer overbalances. Thus, among other contributors to peak broadening, mass transfer resistance, described as the term C in the van Deemter equation, represents the major obstacle to achieving maximum separation performance in peptide LC separations [11].

Regarding the acid-base properties of peptides, tryptic peptides typically have at least two chargeable groups – the amino group at the N-terminus and the carboxyl group at the C-

terminus. As side chains of amino acids may also contain these two moieties, peptides behave as amphoteric molecules with multiple possible pH-dependent dissociation states. Individual dissociation states of a peptide differ in hydrophobicity, thereby retention in reversed-phase chromatographic mode. Thus, the retention of a peptide in a chromatographic column at a certain pH is the sum of the retentions of its possible dissociation states multiplied by their relative abundances. For a robust separation with stable retention time across analyses, the pH of the mobile phase should be at least 1.5 pH units below the lowest or above the highest pK_a value among all chargeable groups in the peptide structure. On the other hand, such sensitivity of retention to pH is an opportunity to perform two-dimensional LC separation with orthogonal selectivity at opposite pH extremities [26]–[28].

Templates of possible peptide structures are not only given by the amino acid composition and their sequence. As proteins undergo post-translational modification, numerous modifications can be identified in protein structures, also at the peptide level. This feature is used in bottom-up proteomic analyses – the protein structure is investigated using peptides in the role of protein fragments. There are more than 400 *in vivo* occurring post-translational modifications (PTMs) located on the side chains of amino acids or the N-terminus of a protein [29]. The most frequently studied PTMs are phosphorylation, acetylation, glycosylation, ubiquitination, methylation, oxidation, formylation, and succinylation. PTMs play a key role in numerous biological processes by changing the protein structure and dynamics. These modifications affect a wide range of protein behaviors and characteristics, including enzyme function and assembly, protein lifespan, protein-protein interactions, cell-cell and cell-matrix interactions, molecular trafficking, receptor activation, protein solubility, protein folding, and protein localization [29]. In therapeutic proteins, PTMs play an important role as well since their efficacy and safety are dependent on the expression of certain modifications (for a review of the PTM roles in monoclonal antibodies, see [30]). That is why these modifications, also belonging to critical quality attributes (CQAs), represent key targets for proteomic analyses in the quality control of biopharmaceuticals [31].

Besides *in vivo* generated modifications, certain changes in peptide or protein structure may occur artificially during sample preparation, storage, and analysis [9][32]. Such artificial modifications are often referred to as post-isolation and the modified peptides – as artifacts. The most known of them are Met oxidation, Asn deamidation (beginning with succinimide intermediate formation mentioned as ammonia loss, followed by conversion either into Asp or isoAsp), pyroGlu formation from the N-terminal Glu and Gln, and Asp dehydration (*see Scheme S1 in Supp. Materials*). The conditions accelerating the modification process had been extensively studied for most of the mentioned reactions [33]–[40]. Mostly, they involve high temperatures, the presence of oxidants or metal traces, and specific pH ranges. Low pH and elevated temperature were also shown to promote non-enzymatic cleavage specific to the C-terminus of Asp, as well as to the N-terminus, but with slower kinetics [14][41]. The extent of modification strongly correlates with the intensity of a condition, e.g., the value of temperature or pH and the time that peptides are exposed to described conditions.

For proteomic analyses, the artificial modification leads to several undesired consequences. First, as a modified peptide is generated from its unmodified form, the concentration of the unmodified form decreases, along with the chance of its identification. In other words, instead of the initial high concentration of the unmodified peptide, there are two (or more) peptides of the same sequence all present in lower concentrations, which consequently reduces the probability of identification of at least one peptide covering this sequence segment. Secondly, the presence of several peptide forms with the same sequence does not provide additional biological information and does not result in the identification of a new protein. Hence, the sample becomes more complex without providing new biological information. When the number of simultaneously identified peptides is limited by the intrinsic capabilities of an analytical technique, the modified form could "occupy" the spot in the list of identified peptides, which would belong to another wanted peptide of a different sequence. Thus, artificial modifications may compromise the number of identified peptides and overall analysis productivity. Furthermore, a specific subset of artificial modifications formed during sample preparation or analysis can mimic *in vivo* protein modifications, hampering their characterization [7][8]. In the case of biopharmaceuticals, artifact formation may compromise the detection and accurate quantification of modifications formed during production or storage [9][36][38]. Due to this, post-isolation modifications have become a frequent topic in the proteomic field, which has led to the development of preventative measures, such as the implementation of sample preparation protocols generating a reduced number of artifacts, especially in the quality control of biopharmaceuticals [42]–[47], and optimization of analytical methods with emphasis on reduced artifacts [3].

3.2. Application of Liquid Chromatography Hyphenated to Mass Spectrometry in Analysis of Proteins

Liquid chromatography hyphenated with mass spectrometry represents a leading analytical technique in bottom-up proteomics. Being unprecedentedly sensitive and productive, highly sophisticated LC-MS workflows nowadays allow for the identification of thousands of peptides and, subsequently, proteins from one sample [48]–[51]. The productivity of LC-MS-based methods is widely utilized in numerous applications: from targeted quantitative analyses of specific proteins of interest as biochemical markers of diseases to exploratory proteomics that focuses on untargeted protein mapping of entire cells or tissues. LC-MS also plays an essential role in the quality control of therapeutic proteins [52], which undoubtedly belong to one of the most innovative drugs.

A typical proteomic bottom-up workflow relies on protein digestion, followed by chromatographic separation and peptide characterization using a tandem mass spectrometer [20]. The acquired MS/MS spectra are searched against a spectral library generated from the protein sequences of interest under specified conditions. The entire analysis results in a pool of peptide-spectrum matches (PSMs) representing identified peptides. If the peptide sequence is long enough, it becomes a fingerprint enabling the identification of a certain protein or at least a protein family sharing the same sequence segment. Alternatively, protein characterization can be performed via a middle-up or middle-down approach, based on the

analysis of protein subunits or polypeptides, or using a top-down approach, which analyzes proteins at their intact state [53]. Additional information about protein structure may also be obtained from the amino acid analysis, which requires total hydrolysis of peptide bonds.

In exploratory bottom-up proteomics, one of the main goals is to achieve the highest number of identified peptides (and then proteins), which describes the coverage of the sample proteome within the shortest analysis time. Great coverage and depth of exploration are achievable in the case of efficient peptide separation and sufficient method sensitivity. To simplify the task of the LC part, it must separate peptides entering MS into narrow and intense peaks, homogeneously distributed over the elution window. The narrower the peptide bands, the fewer peptides simultaneously enter the ion source. Consequently, a larger portion of them gets a chance to be sequenced. Also, the narrower the bands, the more concentrated they are and the more intense the resulting peptide peaks. This underlies improved method sensitivity. This is how the efficient separation increases the number of identified peptides directly and via improved method sensitivity. Achieving efficient peptide separation enables the maximum exploitation of the MS instrument capabilities. Subsequent success is dependent on the parameters of data acquisition and evaluation of generated spectra. The task of the mass spectrometer is to acquire spectra of good quality for the highest number of peptides in the sample. The last challenge is to set suitable search parameters for the pool of acquired spectra so that the maximum of them is correctly assigned to peptide sequences and proteins.

3.2.1. Sample preparation

The task of sample preparation in the bottom-up approach is to generate a peptide set from a protein sample (Figure 1). First, to access peptide bonds to a cleaving agent, proteins should be denatured using an agent with detergent activity. Denaturing agents, such as guanidine, urea, or sodium deoxycholate, unfold and alter protein structure, disrupt non-covalent interactions, and promote hydrophobic protein solubilization, altogether increasing the efficiency of subsequent procedures [54]. The next step is a reduction of disulfide bonds, typically performed with dithiothreitol, tris(2-carboxyethyl)phosphine hydrochloride (TCEP), or β-mercaptoethanol, which is essential for subsequent blocking of free thiols with iodoacetamide, chloroacetamide, or S-methyl methanethiosulfonate. All blocking agents donate the alkyl group that attaches to the free sulfhydryl groups, preventing them from reverse disulfide bond formation. Alkylating agents differ in required concentration, incubation conditions, reactivity, off-target activity, and the tendency to promote other artificial modifications [19][55][56]. Denatured, reduced, and alkylated proteins may be cleaved with chemical agents (cyanogen bromide, 2-nitro-5-thiocyanobenzoate, hydroxylamine [57]) or, more often, enzymes, such as trypsin, Lys-S, Lys-N, chymotrypsin, or ArgC [58]. The most preferred cleavage method is tryptic digestion, which generates peptides of optimum length, mostly not exceeding 5-6 kDa. Trypsin cleaves at the C-terminus of lysine and arginine if not followed by repeated amino acids with basic side chains, proline, or certain PTMs [59][60]. The enzyme selection depends on the desired peptide length, preferred terminal amino acids, and, generally, on the task of the experiment.

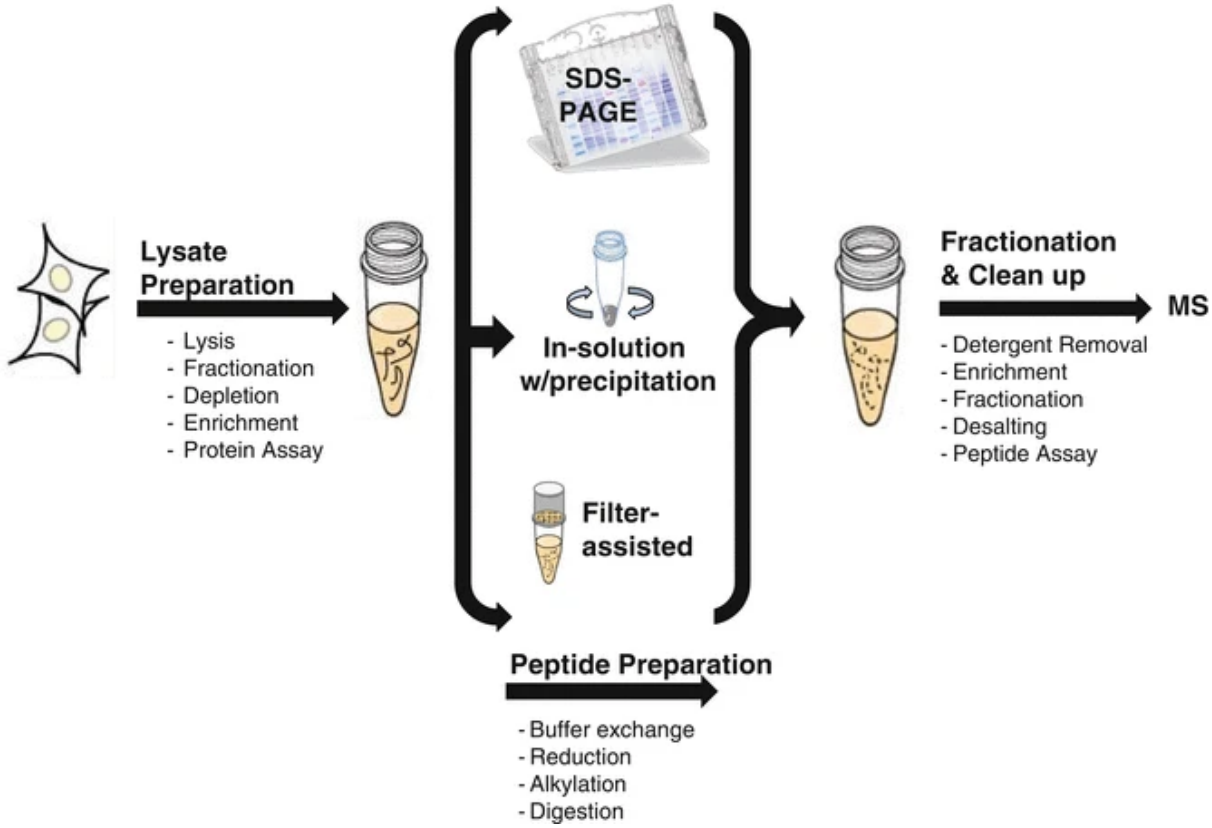

Figure 1: General sample preparation workflow for biological samples (adapted from [20]). There are many options for extracting proteins from tissues and cell lysates, protein fractionation, enrichment, and digestion into peptides for MS analysis.

Alternatively, peptide mapping protocols may be performed under non-reducing conditions if the experiment is aimed at the positions of disulfide bonds in the protein. These protocols skip reduction and thiol blocking and digest proteins right after the denaturing. Furthermore, blocking free thiols was generally shown to be a potentially skippable step, provided that the concentration of the reducing agent is sufficient for maintaining the sulfhydryl groups in a reduced state within digestion [61].

After digestion, the sample may require the removal of small-molecule contaminants because of their incompatibility with MS detection. For complex peptide samples, typically whole-cell or tissue digests, fractionation is also considerable in the effort to decrease the number of peptides that are to be separated in one run. If the complex sample is analyzed without the fractionation, such analyses are referred to as single-shot.

Each step of the sample preparation requires specific conditions to ensure the quantitative course of a reaction. The main condition is to maintain sufficient concentration of a reagent in the mixture and follow the recommendations of the incubation time or temperature. pH adjustment is also necessary for several steps. For instance, proteases mostly require a pH slightly above 8. For some enzymes, it is also essential to avoid the co-presence of denaturing, reducing, or alkylating agents at high concentrations by buffer exchange to preserve their intrinsic activity. It is based on the simple fact that enzymes are proteins as well as the sample proteins. All procedures should be carried out at the lowest possible temperature in the shortest possible time to minimize artificial modification [9]. Unfortunately,

it may compromise the efficiency of digestion. Therefore, certain trade-offs between these two opposite issues must be found during the optimization of sample preparation protocols. Regarding the acidity of the reaction solution, it becomes even more complicated with 3 variables: proteases require a pH of >8, but this pH also promotes deamidation of Asn. On the other hand, it is undesired to lower pH because of the risk of Asp dehydration, pyroGlu formation, and other modifications. As the topic had become more complicated with the rise of interest in artificial modification, numerous studies were conducted to find an optimal procedure. Mostly, these studies investigate the impact of selected reagents and incubation conditions. Also, numerous commercial solutions currently exist on the market [62]–[65].

The final sample solvent is the last considerable variable. Water is preferable both for dissolution and analysis since most proteomic LC separations are performed in the reversed-phase mode. The sample should not contain a high fraction of acetonitrile to prevent peak distortions, but the addition of a small amount is recommended to avoid precipitation of most hydrophobic peptides. To prevent the irreversible adsorption of peptides onto the vial surface, the addition of 0.001% 20 000 g/mol polyethylene glycol (PEG) may also be necessary [66]. Practitioners should also avoid sample dissolution in aqueous 0.1% formic acid as it can result in artificial formylation at the N-termini of peptides [33]. For the prevention of sample degradation and artifact formation during sample storage, the sample should be stored in a freezer at a low temperature until transferred to a cooled LC autosampler [67].

3.2.2. Separation conditions

Most separations in LC-MS-based proteomics are performed in the reversed-phase mode [11]. It is because of its robustness, reproducibility, ease of method development, and balanced hydrophobicity of peptides compared to the hydrophobicity of common stationary phases. Other separation modes may be beneficial for obtaining orthogonal selectivity. The second most mentioned mode is hydrophilic interaction chromatography, which finds its application mainly in the characterization of glycans. The first-choice stationary phase ligand in the reversed-phase mode is octadecyl (C_{18}). Alternatively, if an experiment requires lower retentivity of the stationary phase, octyl (C_8) or butyl (C_4) ligands can be considered. The vast majority of studies traditionally involve particulate homemade or commercial columns packed with silica-based totally porous 2-3 µm particles [11]. Superficially porous particles or sub-2µm particles, being the main advances in stationary phase technology over recent decades, are rather seldom used despite their indisputable advantages. However, in the field of particle chemistries, such novelties as Charged Surface Hybrid (CSH, Waters) or similar products from Agilent or Phenomenex are not that rarely mentioned [68][69]. CSH particle chemistry offers positively chargeable ligands incorporated at the particle surface for the reduction of secondary interactions with charged silanols and reduced signs of overloading when a low-ionic-strength mobile phase is used. Common stationary phases also include Acclaim PepMap (Thermo Fisher Scientific), Ethylene Bridged Hybrid (BEH, Waters), and High Silica Strength (Waters). They differ in retentivity even if the same C_{18} ligand is used [10][70].

Particle pore size. Since peptides have greater hydrodynamic diameter than small-size molecules, they require corresponding adjustment of the particle pore size. 99% of the active chromatographic surface is located in particle pores. Therefore, if the pore surface is not accessible to a peptide, it may suffer from poor retention and peak broadening because of

fewer interactions with the stationary phase ligands [11]. Additionally, if the particle pores are not large enough, the secondary size-exclusion retention mechanism appears, as well as the worsened diffusion between the internal pore space and the interstitial space outside the particle, resulting in increased resistance to mass transfer. Both issues then manifest as peak broadening and/or tailing. On the other hand, larger particle pores can lead to decreased column retentivity because of reduced surface area. If we consider peptides generated by trypsin as the protease of choice, the hydrodynamic diameter of tryptic peptides may reach 20-25 Å. Guided by the rule that the pore size should be 3- to 5-fold larger [71], the optimum pore size starts at 100 Å. Larger sizes may be beneficial for the separation of samples digested with enzymes that generate longer peptides, such as Lys-C.

Inner column diameter. The inner diameter of the column defines the largest number of the LC-MS system volumetric characteristics. The nomenclature of columns based on their i.d. and the terminology of related flow regimes have not been unified, but for this work, the text below will follow the classification proposed by *Lenčo et al.* (Figure 2) [11]:

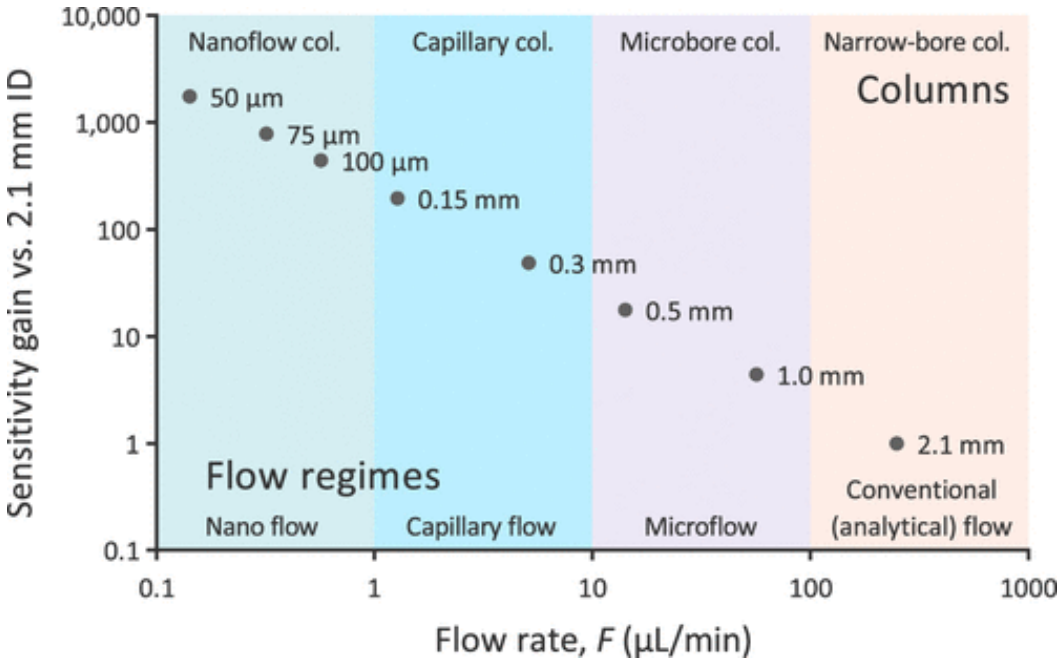

Figure 2: Classification of column formats and flow rate regimes proposed by *Lenčo et al*, appended with corresponding sensitivity gains in comparison to a hypothetical 2.1 mm i.d. column.

The inner column diameter determines method sensitivity, dictates the mobile phase flow rate, injected mass of peptides, dimensions of capillaries up and downstream of the column, and the volumetric characteristics of the ion source of the mass spectrometer. As proteomic analyses usually deal with small sample quantities and the sample components are present in a wide range of concentrations [72], proteomics has been almost dogmatically linked to nanoflow columns. They provide the lowest sample dilution ratio, which is beneficial for mass spectrometers with a traditional electrospray ionization source, behaving as a concentration-dependent detector [73]. Despite this key advantage of the nanoflow regime compared to the micro- and conventional-flow ones, nanoflow columns suffer from lower robustness, sample throughput, and shorter lifetimes. Also, the narrower the column, the less

homogenously it is practically packed, which negatively influences the eventual separation performance. Moreover, nanoLC requires specific technical solutions in the hardware to deliver accurate gradients at sub µL/min flow rates and enable the injection of volumes several times exceeding the nanoflow column volumes [74]. Also, troubleshooting in nanoLC is more challenging than in the conventional-flow regime because of its slow responsiveness. That is why wider columns gain interest in various applications [15][17][18]. A recent study demonstrated that the increase in the sample amount needed to approach sensitivity common for nanoLC while operating in the microflow regime is significantly lower than that predicted [14]. In the sphere of biopharmaceutical quality control, where the sample quantity is relatively unlimited, and the protein concentration is simply adjustable, microbore and narrow-bore columns represent the dominant column formats.

Column length. The second parameter describing column dimensions is the column length. In proteomics, it varies from 5 to approximately 75 cm. Longer columns improve separation performance and the number of identified peptides, particularly when long gradient methods are used [2][75]. On the other hand, longer columns suffer from axial heterogeneity of packing, prolong the retention time of analytes, and require more time for column equilibration to initial gradient conditions [76]. These negative effects collectively diminish the sample throughput and the peak capacity per total analysis time [77]. The accompanying negative effect of longer columns is the higher back pressure. However, the column can be operated under a higher temperature or reduced flow rate, both being beneficial for the number of identified peptides.

Connecting capillaries. The column dimensions also define the volume of capillaries linking the sample loop and the detector. The narrower the column, the smaller the volume of connecting capillaries should be to preserve the separation performance of the column. Ideally, connecting capillaries should be as small as possible, but the selection is limited by the generated back pressure. The selection of the capillary installed upstream of the column is less critical because, due to their high parameter S, peptides are anyway refocused after the injection at the head of the column, provided that the initial mobile phase is weak enough [11].

Mobile phase. Most proteomic studies involve water-acetonitrile mobile phases, with rare exceptions for methanol. The pH of the mobile phase for bottom-up proteomic analyses is traditionally acidic because it does not hydrolyze the silica support of the particulate stationary phase and keeps surface silanols in the undissociated state, preventing them from unwanted secondary interactions with protonated analytes [11]. If all carboxyl groups in a peptide set are kept at a pH lower than the lowest pK_a by at least 1.5 units, it guarantees the undissociated state of all of them. This ensures the reproducibility of retention time and mitigates metal chelating tendencies, which may manifest as peak distortions. Moreover, acidic pH facilitates the protonation of peptides during electrospray ionization, making it ideal for the downstream MS analysis of peptides with basic functional groups in the positive mode [78]. The first-choice acidifier is 0.1% formic acid as it is volatile, i.e., MS-friendly, and does not suppress ionization as does trifluoroacetic acid (TFA) [79]. However, formic acid, being beneficial for LC-MS, is not the best option among these two acids in LC-UV. Formic acid has only a limited ability to form ion pairs in the concentration of 0.1%, which does not allow for efficient prevention of secondary interactions with residual charged silanols. The peak shape

of peptides separated in such a low-ionic-strength mobile phase shows signs of overloading. However, this issue became less significant with the introduction of novel particle chemistries such as CSH. This also enabled the reduction of the concentration of formic acid in the mobile phase to mitigate residual ionization suppression that is still noticeable when 0.1% formic acid is used [80]. Compared to TFA, formic acid also provides a higher pH, which may result in undesired partial dissociation of certain peptide carboxyl groups with a lower pK_a. To summarize, TFA enables more efficient and reproducible separation than formic acid, which defines its status in LC-UV analyses. On the other hand, TFA significantly suppresses the ionization of peptides in the ion source due to strong ion-pairing properties, which makes TFA inapplicable in LC-MS and makes formic acid the preferred option. Interestingly, the concentration of formic acid was also shown to influence peptide retention on common stationary phases, such as CSH and BEH C_{18} (Waters) [80]. When the concentration of formic acid is reduced, pH increases. This leads to partial ionization of certain peptide carboxyl moieties. Charged carboxyl groups interact with the positively charged surface of the CSH stationary phase. These secondary ionic interactions increase peptide retention in the CSH phase [81]. The opposite result may be observed in separations with reduced concentration of formic acid when the BEH stationary phase is used.

Auxiliary mobile phase additives. Besides the major components, the mobile phase can contain auxiliary additives with specific roles. Regarding, for example, the chelating properties of certain amino acid residues, it may happen that the pH maintained by weak 0.1 % formic acid is not low enough to keep all carboxyl groups in the undissociated state. These charged groups then behave as chelators for metals, including those present on the internal surface of the column cylinder. Peptides interact with the metal surface and consequently suffer from peak tailing. Antichelating additives, such as acetylacetone, citrate, and medronic acid, can be added in low µmol/L or mmol/L concentrations to the mobile phase to improve the peak shape of peptides with strong chelating properties [82]. Antichelating additives also reduce in-column Met oxidation associated with metal traces [35]. Aiming at the same issue of secondary interactions, Waters developed a dedicated product line of columns with internal coating, which prevents the mobile phase from contact with the metal surface of the column (MaxPeak High-Performance Surfaces Technology, product line of Premier columns) [83].

Gradient elution. Due to the special retention behavior of peptides, proteomic separations must necessarily be performed using gradient elution. Gradient methods usually start at a small percentage of a strong mobile phase component, which increases with a linear or segmented course up to a final value, followed by the column wash and an equilibration step. The weaker the initial mobile phase, the higher the probability of retention and separation of the least hydrophobic peptides that leave the column at the beginning of the elution window. A short isocratic hold at the initial mobile phase composition between the injection point and the beginning of the gradient can be added to separate non-retained small-size contaminants from the peptide fraction. However, if the gradient delay time of the instrument configuration is long enough, it *de facto* substitutes this isocratic step. To avoid ion source contamination by non-retained compounds, the mobile phase flowing out of the column can be diverted to waste at the beginning of the run for a time slightly longer than the column dead time.

Gradient length varies from several minutes to 4 hours, which is an unmet situation in the analysis of small molecules. The setting of gradient time primarily depends on the sample complexity. The more complex the sample, the longer the gradient duration should be to keep a reasonable number of peptides eluting simultaneously [75]. However, this tool only works to a limited gradient time, meaning that the number of identified peptides from the given sample will stop increasing with gradient extension after reaching this limit [11]. Moreover, this dependency is valid only for sufficiently long columns. As gradient length defines the time peptides spend in the column, it directly affects the extent of the artificial modification process, yet it is more critical if the column is maintained at a high temperature [3].

3.2.3. Detection

Bottom-up proteomics is traditionally linked to MS detection. Compared to UV or charged aerosol detection, MS detection provides an additional dimension of information about peptide structure. The single knowledge of retention time and the quantity of analytes provided by the mentioned UV and charged aerosol detectors remains sufficient, for instance, in simple peptide mapping of biopharmaceuticals in their quality control. However, even in this application, peptides must be first sequenced by the tandem mass spectrometer. Along with the rise of MAMs for the characterization of therapeutic proteins, the interest in UV detection is progressively decreasing. MAMs exploit the universality of MS detection and focus on multiple CQAs in protein structure, substituting traditional single-attribute methods (for a recent review, see [16]). Besides providing information about peptide structure, MS detection is undoubtedly superior in sensitivity and the ability to characterize multiple analytes simultaneously. That is why MS detection holds a monopoly in exploratory proteomics and quantitation of low-abundant peptides in complex samples. On the other hand, due to the robustness and ease of use of the UV detector, its utility should not be overlooked in cases when the identification of peptides is not required, peptides are effectively separated and provide a sufficient signal-to-noise ratio.

The MS characterization starts with the ionization of peptides and evaporation of the mobile phase using electrospray ionization (ESI source), mostly in positive mode. Peptides are introduced in the ESI via a needle of the dimensions that should be selected based on the dimensions of the column and the flow rate [14]. Also, the depth of the ESI probe must correspond to the applied flow rate. The performance of the ion source can be improved by the introduction of heated auxiliary gas – such an ion source is referred to as Heated ESI (HESI). The parameters of the ion source should be optimized to achieve efficient spray formation and the highest intensity of peptide peaks. Numerous software products offer automatic adjustment of these parameters according to the mobile phase flow rate.

Charged peptides then pass through MS1 filtering, fragmentation, and detection in a high-resolution tandem mass analyzer. Typically, it is a time-of-flight analyzer with a prepended quadrupole or an electrostatic orbital ion trap. Only these instruments combine high resolution and fast scan frequency [84]. The fragmentation is induced by collisions of ions with neutral gas molecules using additional electric potential. This technique is called collision-induced dissociation. One of the derivations of this technique is higher-energy collisional (or formerly known as “C-trap”) dissociation (HCD). This derivation is available in specific Orbitrap Thermo Fisher Scientific mass spectrometers.

For untargeted exploratory proteomics, there are two basic data acquisition mods: data-independent acquisition (DIA) and data-dependent acquisition (DDA). The latter approach used to be the most popular in the field. However, along with the advances in spectra evaluation [85][86], DIA has gradually become a leading approach in numerous applications. One of the exceptions is PTM analysis, where DDA still holds a monopoly. DDA is based on the selection of a limited number of the most intense precursor ions (TopN, N is mostly 3 to 20) that exceed the given intensity threshold, provided that they are not included in the exclusion list or dynamically excluded from fragmentation at the moment of MS1 filtering. Precursors are selected during a first-in-the-order survey MS1 scan. The selected precursors are then sequentially fragmented during MS/MS events. The total cycle time is the sum of (i) the time of precursor ions accumulation (termed as injection time) for the survey MS1 spectrum, (ii) MS1 spectrum acquisition, (iii) online software evaluation of the precursor list, (iv) accumulation of a single precursor ion for fragmentation, and (v) MS/MS spectrum acquisition. The total duration of the last two steps is multiplied by the number of precursors. The cycle time also includes interscan delays and the time needed to switch the acquisition settings. Instead of setting ion accumulation times, some instruments offer the setting of a target count of ions (automatic gain control, AGC) as a tool for tuning target ion quantities. The count of accumulated ions and the spectra acquisition time define the peak intensity and the quality of spectra, which affects the probability of spectrum assignment to a correct peptide sequence. However, if a method involves the selection of numerous precursors and long times of ion accumulation or spectra acquisition, the total cycle time increases, which leads to a drop in scan frequency, resulting in fewer identified peptides [84]. A too-short cycle would oppositely lead to spectra of poor quality with low signal intensity, compromising method sensitivity. For maximum productivity, other important parameters must be balanced:

- resolution – the higher the resolution, the higher the mass accuracy, but the longer the spectrum acquisition time (valid for Orbitrap instruments)
- intensity threshold for MS/MS event triggering – the lower the threshold, the higher the probability of fragmentation of low-abundant peptides, but also the more probable the fragmentation of single-charged background ions if a single charge state is not generally excluded from fragmentation.
- list of precursors permanently excluded from fragmentation regardless of their intensity (exclusion list) – to avoid fragmentation of background ions.
- time during which the same precursor will not be fragmented repeatedly (dynamic exclusion) – to avoid the generation of multiple spectra for the same peptide. Alternatively, dynamic exclusion time can be set so that the next spectrum of the given peptide is acquired at the peak apex to obtain a spectrum of better quality.
- apex trigger – to obtain an MS/MS spectrum at the LC peak apex with the highest intensity.
- m/z window of precursor isolation – the too narrow window will result in non-quantitative isolation of a precursor, too wide – in co-isolation of multiple peptides, leading to a chimeric fragmentation spectrum.
- isolation m/z offset – to cover an isotopic cluster as well as the monoisotopic peak.

- permanent exclusion of certain peptide charge states - to reject individual charge states or undetermined charge states as precursors for MS/MS scans.
- exclusion of isotopic peaks from isolation
- isolation of the most intense peptide charge state
- chromatographic peak width – expected average peak width at half height used by certain software products in the calculation of the dynamic exclusion and AGC target in case of automatic setting.
- normalized collision energy – the higher the collision energy, the more intense the fragment ions, and the lower the remaining intensity of a parent peptide. However, too high collision energy may result in an overfragmentation with a high abundance of low-mass fragments. The normalization means that the collision voltage is adapted for m/z and the charge state of individual peptides so that the eventual collision energy transmitted to different peptides is roughly equal and, therefore, can be set universally [87][88].

In contrast to DDA, DIA avoids the detection and selection of individual precursor ions via co-selection and co-fragmentation. Convoluted or multiplexed MS2 spectra are generated without explicit association between each single precursor and its corresponding fragments. As a result, DIA requires more sophisticated post-acquisition data analysis compared to DDA. On the other hand, DIA is unbiased by precursor intensity, and its performance is less vulnerable to the presence of multiple co-eluting peptides and, generally, to high sample complexity. DIA also has a wider dynamic range, which enables more accurate quantitation. Finally, it provides a higher probability that the given precursor will be again fragmented in replicated analyses of the same sample.

3.2.4. Data evaluation

Because of enormous spectral complexity, data evaluation in proteomics is routinely performed by dedicated search software products [89]. The inputs for the assignment of spectra to peptide sequences are a pool of acquired spectra containing fragmentation patterns characteristic to specific peptide sequences and a spectral library that consists of predicted spectra corresponding to candidate peptide sequences generated under specified parameters. Alternatively, acquired spectra can be compared to the spectra available in databases of experimentally acquired spectra. The spectral library is created by the software, which “digests” downloaded protein sequences (usually as a file of FASTA format) based on preset parameters. The common parameters are enzyme type, enzyme specificity (fully or semi-specific cleavage, other options available), allowed number of missed cleavages along one peptide sequence, fragmentation type, mass tolerance for precursors and fragments, disulfide bridge inclusion, etc. The spectral library is traditionally enriched with possible modifications in peptide structures: fixed modifications (peptide sequences free of a certain fixed modification on a specified amino acid are not considered) and variable modifications (both modified and unmodified peptide sequences are included in the search) with the specification of their occurrence frequency. Typically, modification lists include modifications obligatory from the biological point of view (PTMs) and the sample preparation- or analysis-related artifacts. To control the combinatorial explosion of the number of sequences modified in

multiple ways, the software usually provides the setting of the maximum of variable mods. Quantitation-oriented products, such as Skyline, also provide the setting of post-acquisition MS1 filtering, e.g., possible charge states of a precursor and an interval of retention time around the MS/MS identification time, which is used for filtering an identified precursor [90]. The less strict the search parameters, the larger the generated spectral library, and the more peptides become potentially identifiable. On the other hand, it increases the computational load and the search time. Therefore, the search parameters should be set according to the experiment's aim to identify the set of peptides of interest preferentially. Also, relaxed parameters of mass tolerances usually lead to a higher number of PSMs, but the reliability of identification is logically diminished. The search engine compares acquired spectra with the spectra from the spectral library. The search results in a pool of PSMs, which cover a certain portion of acquired spectra. Each PSM is scored according to the similarity of the spectra. PSMs are subsequently ranked based on the matching score. The software selects the best-scoring peptide sequence as the most likely true sequence.

Alternatively, peptide sequence can be extracted directly from the acquired spectra, i.e., without referring to an external spectra database or a generated spectral library (*de novo* sequencing approach). This approach is based on the calculation of the mass differences between the next and the previous peptide fragment. The calculated mass differences are then assigned to individual amino acid residues, and the calculation continues amino acid by amino acid. There are also hybrid approaches, such as those based on the extraction of short sequence tags of 3-5 amino acids combined with database searching [91][92].

As the absolute correctness of PSM *a priori* cannot be guaranteed, PSM sets always contain a certain portion of false identifications. Several measures were introduced for the characterization of the false PSM abundance. In the case of large datasets, the most used statistical confidence measures are false discovery rate (FDR, percentage of false peptides in an entire set of PSMs) as a summary statistic for the entire collection of PSMs and posterior probability (percentage of true peptides among all PSMs) [91]. At the peptide level, FDR ≤1% is considered the standard tolerated error rate. There are several strategies for FDR estimation. The most common is the target-decoy strategy [93]. This strategy requires that experimental MS/MS spectra are searched against a target database of protein sequences appended with the reversed or randomized sequences of the same size. The basic assumption is that the probability of a match to decoy peptide sequences (decoy PSMs) and false matches to sequences from the target database (target PSMs) are roughly equal. In the second step, PSMs are filtered using various score cut-offs. The FDR corresponding to each cut-off is estimated as the number of decoy PSMs divided by the number of target PSMs with scores above the given score cut-off. Provided that the sizes of the target and decoy database are equal, the number of false target PSMs can be estimated through the number of decoy PSMs. The pipelines usually offer a selection of a tolerated FDR level, and the search engine calculates the corresponding score cut-off that serves as a boundary between accepted and unaccepted target PSMs. The higher the FDR level, the lower the score cut-off, and the more PSMs are eventually accepted, but the higher number of them are accepted being potentially falsely identified. Alternatively, there is an option to select the threshold number of decoy PSMs for a dataset, and the score cut-off is set at the score of the lowest-ranked decoy PSM; FDR is then calculated from the number of target and decoy PSMs [92].

Protein assignment is performed via correlation of protein sequences with the identified peptides. The longer the sequence, the more reliable the assignment, and the lower the probability that the peptide might be “shared” with the other protein. The high number of identified peptides per protein also increases the confidence in protein identification. The calculation of FDR is also applicable at the protein level and is performed analogously: the PSM score is replaced with the protein score, the target database is enriched with randomized sequences of target proteins of the same size, and the protein score cut-off is selected so that the FDR is controlled at the desired level. Both strategies can be fused in the two-dimensional FDR, which takes features of FDR calculation at both levels to preserve the low level of false positives while not discarding extensive sets of false negatives, which would be otherwise accepted under the manual human expertise [94].

3.3. Role of Column Temperature

The column temperature represents an exceptionally cost-effective and powerful means that can substantially improve peptide separation, which increases the number of identified peptides from a complex sample [3][5][6]. Unfortunately, its benefits are generally overlooked in bottom-up proteomics, perhaps due to the requirement of additional LC accessories or doubts about the stability of stationary phases. The most noticeable effects of elevated column temperature are undoubtedly decreased retention and lower back pressure. The lower back pressure results from the decreased viscosity of the mobile phase passing the column. This is a typical motivation for using an elevated temperature in proteomic analyses, particularly when long columns packed with sub-2µm particles are used. Its effect on the peptide diffusivity and their adsorption-desorption kinetics is less recognized by the practitioners yet more important. Slow diffusion and lower adsorption-desorption rate of peptides lead to the fact that flow rates typically used in proteomic LC-MS analyses are far above the van Deemter optimum, i.e., in the range where the resistance to mass transfer (C term in the van Deemter equation) is the dominant contributor to the in-column band broadening. The peptide diffusivity can be enhanced by elevated temperature directly and indirectly via the decreased mobile phase viscosity. In turn, faster diffusion and an enhanced sorption rate improve the mass transfer of peptides, which is particularly important for fully porous particles [14]. As a result, the van Deemter minimum shifts to higher flow rates, and the van Deemter plot flattens at higher column temperatures. This manifests as narrower and more intense peptide peaks eluted at the constant flow rate.

The elevated temperature has also been shown to enhance the recovery of peptides, thus minimizing their carry-over [95]. This applies particularly to hydrophobic peptides [96]. Also, the chromatographic behavior of peptides containing proline-proline bonds can principally profit from elevated temperature because of their very slow cis-trans isomerization kinetics [97]. Finally, higher temperatures increase the elution strength of the mobile phase, which reduces the percentage of the organic solvent needed to elute peptides from a column. Thus, reversed-phase chromatography at elevated temperatures is “greener” chromatography compared to separation at lower column temperatures, provided that the gradient shape is properly optimized [6].

On the other hand, high temperature is a common promoter of artificial modification *(see section 3.1. Peptides)*. Therefore, a heated analytical column percolated with a typically acidic mobile phase literally becomes a chemical reactor, especially if long gradient methods are applied. Thus, the potential complications described in that section are also valid for high-temperature LC-MS of peptides, besides non-optimized sample preparation or storage. If a practitioner intends to profit from the advantages of elevated column temperature, it requires awareness of the potential negative consequences [3]. The basic measure that should be introduced is an adjustment of MS data search parameters with emphasis on the presence of modified peptides in the pool of acquired MS/MS spectra. Along with common modifications, such as N-terminal acetylation and Cys thiol blocking, variable modifications mirroring specific degradation reactions should be included in the parameters determining the theoretical list of peptides that are to be searched for a match with acquired spectra. To mitigate the issue arising from the non-tryptic Asp-specific cleavage, semi-tryptic cleavage should be applied as well. If the search parameters remain unadjusted, and the only present form of a peptide is the modified form, this peptide and, subsequently, this segment of the protein sequence will not be covered.

Another consideration should be given to the gradient time. Fast and short gradients will profit from elevated column temperature, as its benefits overcome the degradation extent, which is not that significant in short analyses. However, if a long gradient is considered, a practitioner should find a trade-off between the increase in peak capacity due to gradient time extension and a decrease in the number of identifiable peptides due to long exposition to low pH and high temperature. For extremely long gradients, the application of elevated column temperature may even decrease the number of identified peptides. This number, because of its normalized nature, can be used as a universal analysis output for monitoring method performance when gradient time and column temperature pass through the optimization process [3]. For experiments relying on the intactness of peptide structure, the lowest reasonable column temperature must be applied.

3.4. Trap-Elute Setup

Most nanoLC systems mentioned in proteomic studies exploit the so-called trap-elute setups [11]. Compared to the conventional direct injection configuration, trap-elute systems include a trap column introduced between the autosampler and the separation column. Upon injection, the flow from the trap column is diverted to waste for the time needed for sample loading and a short wash. Then, it is switched towards the separation column at the beginning of the gradient method. Trap columns are usually short and have larger inner diameter than separation columns. They are also often packed with larger particles (typically 5 µm in diameter) to reduce back pressure generated during the sample loading at a high flow rate.

The main motivation for the introduction of the trap-elute setup in nanoLC is to shorten the time of sample delivery from the autosampler to the separation column [10][98]. No less important, this setup enables the injection of large sample volumes, which may even exceed the volume of the separation nanocolumn, with a preserved linear increase in signal response with increasing sample volume. In the case of direct injection, high sample volumes may cause long gradient delay time and/or peak distortion if the sample contains some portion of an organic solvent, which is often the result of an upstream sample preparation. Trap-elute

systems can be used for online solid-phase extraction of peptides from samples containing small-molecule impurities incompatible with MS detection [99]. The trap column, similarly to the widely used guard columns, can also function as a mechanical sieve to filter out particulates in the sample to prevent column clogging and thus extend the lifetime of the downstream nanocolumn.

The sample is loaded onto a trap column in a weak loading solvent under isocratic conditions. The weak loading solvent prevents peptides from traveling along the trap column, whereas the sample solvent and small-molecule contaminants are flushed to waste. Then, the loading solvent is gradually replaced with a stronger separation mobile phase, and peptides start to elute from the trap column. Provided that the separation column is more retentive, the mobile phase that caused peptide elution from the trap column still enables retention and refocusing of peptides at the head of the separation column. At this point, the separation continues analogously to the direct injection under the gradient elution conditions. The unique feature of peptides underlying the efficient utilization of trap-elute setups is their great S parameter, which enables peptide refocusing. This partially eliminates peak broadening upstream of the separation column. It practically means that the separation performance of the optimized trap-elute setup can be close to the performance of the direct injection configuration, even though it cannot reach 100%.

There are several requirements for the optimization of the trap-elute setup. First, as described above, the retentivity of the separation column must be sufficiently high to ensure peptide refocusing after elution from the trap column. Otherwise, the mobile phase causing elution of peptides from the trap column prevents them from retention at the separation column. If peptides are not retained, they do not fully exploit the intrinsic separation potential of the column and, in extreme cases, may just pass through the column. In this case, the separation column only contributes to peak broadening (as do connecting capillaries) instead of providing efficient separation. Therefore, to fine-tune the difference in retentivity between the two columns, the stationary phases of both should be rationally selected. As it is valid for tubing involved in the direct injection configuration, the requirement to reduce extra-column volumes applies to the trap-elute systems as well. The next requirement is to avoid weakly retentive trap columns. Upon sample loading, the flow is diverted to waste. If the sample contains very hydrophilic peptides, they may elute from the trap column to waste, even in the weak mobile phase. Besides the selection of the trap column retentivity, the loading solvent strength must be as low as possible [100]. To increase the hydrophobicity of the least hydrophobic peptides, the loading solvent may be enriched with an acidifier with strong ion-pairing properties, such as TFA [101]. On the other hand, the too-weak solvent might not be sufficient for the elution of small-molecule contaminants. Therefore, the trade-off between peptide retention and sample clean-up is to be found.

There are several additional parameters controlling sample loading that need to be optimized, such as loading solvent flow rate and time of loading. Also, the retentivity of both trap and separation columns can be tuned via a change in the column temperature [13]. This, logically, requires an external thermostat or a column oven that enables differential heating of compartments. As the retention time of peptides in the trap column (describing its retentivity for the purpose of our study) directly depends on the trap column length, it can also be reduced to reach a shorter retention time, associated with a weaker mobile phase, which still

enables subsequent efficient refocusing at the separation column. Alternatively, the loading and elution from the trap column can be carried out in opposite directions [98]. Such a minor modification dramatically reduces the distance in a trap column that the peptides travel along during their trapping/elution and, hence, reduces the time peptides spend in the trap column under gradient conditions. This can be readily realized by interchanging two connections on the switching valve accommodating the trap column (*Fig. 18 in* [11]). However, this remedy cannot be realized in the alternative vented column setup, which represents an economical version that does not require an additional pump [12].

4. EXPERIMENTAL SECTION

4.1. Materials

4.1.1. Chemicals and consumables

Water – LC-MS grade (VWR Chemicals, France)
Milli-Q water – resistivity 18.2 MΩ·cm (Millipore, USA)
Acetonitrile – Optima LC-MS grade (Thermo Fisher Scientific, Belgium)
Formic acid for LC-MS – purity ≥ 98% (Honeywell Fluka, USA)
Propionic acid – purity ≥ 99.5% (Sigma-Aldrich, Germany)
TFA for LC-MS – purity ≥ 98% (Honeywell Fluka, USA)
Benzonase - 250 UI/µL solution (Sigma-Aldrich, USA)
Tris buffer 1M solution, pH 7.5 (SERVA Electrophoresis GmbH, Germany)
Guanidinium hydrochloride 8M solution, pH 8.5 (Sigma-Aldrich, USA)
Dithiothreitol – purity ≥ 99.0% (Sigma-Aldrich, Canada)
TCEP – purity ≥ 99.0% (Sigma-Aldrich, USA)
Iodoacetamide – purity ≥ 99.0% (Sigma-Aldrich, USA)
L-Cysteine hydrochloride – purity ≥ 99.0% (Sigma-Aldrich, India)
Low-Artifact Digestion Buffer (Sigma-Aldrich, USA)
Trypsin Platinum Mass Spec Grade, 1 µg/µL solution (PROMEGA, USA)
Ethyl acetate – purity ≥ 99.1% (Lach-Ner, s.r.o., Czech Republic)
PEG 20 000 g/mol, 0.1% solution (Sigma-Aldrich, USA)
Set of seven indexed retention time (iRT) peptides – purity ≥ 95.0% (Shanghai Royobiotech, China)
Trastuzumab – Herceptin (Roche, Switzerland)
Aflibercept – Zaltrap (Sanofi, France)
Bevacizumab – Avastin (Roche, Switzerland)
HPLC Prodigy Standard AL0-3045 (Phenomenex, USA)
Pierce Peptide Desalting Spin Columns (Thermo Fisher Scientific, China)

4.1.2. Instruments

An Agilent 1290 Infinity II UHPLC system was used for experiments that did not require the identification of analytes. The column thermostat was equipped with a 1 µL passive preheater assembled on a 0.1 mm i.d. Viper capillary, which connected the autosampler and the separation column. In analyses with the trap column included in the configuration, an additional capillary was installed to connect the trap and separation column. The maximum portion of the capillary connecting the two columns was placed in the thermostat to minimize the risk of thermal mismatch between the separation column and the mobile phase inflowing from the trap column maintained at a lower temperature. For the same purpose, this capillary was additionally attached between heated metal parts of the thermostat. The capillary with the passive preheater and the trap column, in turn, were placed in an external still-air

thermostat. Peptides were detected using a UV detector at 214 nm and a data acquisition frequency of 20 Hz. Instrument control and data evaluation were performed using Agilent OpenLAB software.

LC-MS analyses were carried out using a conventional-flow Vanquish Horizon UHPLC system combined with a Q Exactive HF-X mass spectrometer (Thermo Fisher Scientific). The LC tubing from the autosampler to the separation column included a 0.1 mm × 550 mm Viper capillary and a 0.1 × 380 mm capillary with an active preheater. The Viper capillary and the actively heated capillary were connected through a Viper union, which was replaced with the trap column in analyses with the trap-elute setup. The trap column and the Viper capillary were again placed in the external thermostat. Eluted peptides were introduced into the mass spectrometer through a 0.003 in. spray needle inserted in a HESI-II probe. The ion source parameters for each flow rate applied in the study were set in accordance with those proposed by the Exactive Series Tune software. Detailed ion source settings for each flow rate are specified in the Supporting Information, as well as the settings of the mass analyzer for each experiment (*Tables S1 and S2 in Supp. Materials*). The ionization efficiency in microflow LC-MS analyses of the Jurkat cell protein digest was increased via the nebulization of the eluate using nitrogen saturated with vapors of propionic acid obtained using a simple homemade vaporizer constructed according to the previous publications [3][102]. The instrument was controlled through Xcalibur Software, Exactive Series Tune, and Chromeleon Console. All analyses were run in triplicate.

4.1.3. Columns

Separation columns used in the study are narrow-bore 2.1 × 150 mm and microbore 1.0 × 150 mm Acquity Premier CSH C_{18} packed with 1.7 µm fully porous particles (130 Å, Waters). Candidate trap columns of 2.1 mm i.d. were 30 mm and 10 mm Accucore 150-C_4 columns packed with 2.6 µm superficially porous particles (150 Å, Thermo Fisher Scientific), 5 mm Acquity UPLC Protein BEH C_4 VanGuard Pre-column packed with 1.7 µm fully porous particles (300 Å, Waters), and 5 mm Acquity UPLC BEH C_8 VanGuard Pre-column packed with 1.7 µm fully porous particles (130 Å, Waters). In turn, for the microbore 1.0 mm i.d. separation column, we also examined three trap cartridges purchased from Optimize Technologies with dimensions of 1.0 × 5 mm: EXP Trap Cart 4 µL Opti-Sil C_4 and PLRP-S packed with 5 µm and 10 µm fully porous particles (300 Å) respectively, and a custom cartridge packed with the same particles as in the previously mentioned Acquity UPLC Protein BEH C_4 VanGuard Pre-column. Since VanGuard Pre-columns have male-threaded outlet fittings, they were connected to the capillary, leading to a separation column using low dead volume Viper connectors installed once at the beginning of the study (*not shown in Figure S1*). All columns were conditioned prior to use by at least three injections of a relevant peptide mixture to achieve reproducible peak shapes and retention time.

4.2. Methods

4.2.1. Sample preparation

Preparation of iRT peptide mixture

Aqueous stock solutions of seven iRT peptides (LGGNEQVTR, GAGSSEPVTGLDAK, YILAGVENSK, TPVITGAPYEYR, ADVTPADFSEWSK, GTFIIDPGGVIR, LFLQFGAQGSPFLK – listed in the order of ascending hydrophobicity) were mixed so that the concentration of each peptide in the sample was 0.125 μg/μL. The sample also contained 20% acetonitrile to eliminate the risk of hydrophobic peptide precipitation and 0.001% PEG 20 000 g/mol for prevention of peptide adsorption onto a vial surface. The mixture was initially prepared for stock, divided into aliquots, and stored at -20 °C. Prepared aliquots were thawed before individual experiments and kept within running measurements in an autosampler at 4 °C for no longer than 1 week.

Trypsin digestion of proteins of F. tularensis live vaccine strain and Jurkat human cells

Cell samples processed previously by Dr. Lenčo and Dr. Fabrik were washed and lysed in 2% sodium deoxycholate. Protein concentration was determined using a bicinchoninic acid assay. The volume of a whole-cell lysate containing 1 mg of proteins was incubated with 250 UI of benzonase for 30 min at 37 °C in an environment of 100 mM Tris buffer, pH 7.5. Proteins were reduced in 5 mM TCEP for 60 min at 37 °C, and free thiols were blocked in 15 mM iodoacetamide at room temperature for 30 min in the dark. The thiol blocking was quenched by incubation in 20 mM L-Cysteine under the same conditions. The mixture was then diluted with 50 mM Tris buffer to reach a pH above 7 and reduce the concentration of TCEP. Mass Spec Grade Trypsin Platinum was added in a 1:50 enzyme-protein mass ratio, and the proteins were digested at 37 °C overnight. The digest was acidified with a sufficient volume of pure TFA to reach a pH below 2, which quenched the enzymatic reaction and induced deoxycholic acid precipitation. The precipitated acid was then extracted into ethyl acetate saturated with water. The remnants of ethyl acetate were evaporated in a vacuum centrifuge at 30 °C within 30 min. The digest was then desalted using a Pierce Peptide Desalting Spin Column according to the manufacturer's manual [103]. The eluate containing 50% acetonitrile was dried in a vacuum centrifuge at 37 °C. Dry peptides were dissolved in 0.1% aqueous TFA and 0.001% PEG 20 000 g/mol, divided into aliquots, and stored at -80 °C until analysis.

Trypsin digestion of therapeutic proteins

Lyophilized proteins were dissolved in water, denatured in 6 M guanidinium hydrochloride, pH 8.5, and reduced in 20 mM dithiothreitol for 30 min at room temperature. Cys thiol blocking was not performed. The denatured protein solution was diluted with a Low-Artifact Digestion Buffer containing dithiothreitol so that its concentration in the digestion mixture was 2 mM. After the dilution, the buffer made up more than 80% of the mixture and the concentration of guanidinium hydrochloride dropped to approx. 660 mM. Mass Spec Grade Trypsin Platinum was added in a 1:20 enzyme-protein mass ratio, and the proteins were digested at 37 °C for 2 hours. The digest was acidified with TFA. The final peptide solution also contained 0.001% PEG 20 000 g/mol. The prepared digest was then treated in the same manner as in the previous procedure.

4.2.2. Trap column selection and optimization of analytical conditions

Each 2.1 mm i.d. trap column was initially examined using isocratic separation of small molecule standards (HPLC Prodigy Standard AL0-3045) on Agilent 1290 Infinity II UHPLC system with UV detection. Mobile phase components were 0.05% formic acid in Milli-Q water (component A) and 0.05% formic acid in LC-MS grade acetonitrile (component B). Mobile phase components were prepared using a volumetric flask in an amount adequate for the duration of an experiment and used for no longer than one week. The isocratic methods involved separation at 30 and 40% component B lasting for the time sufficient for elution of all four analytes. The mobile phase flow rate was 300 µL/min and kept constant in all experiments involving 2.1 mm i.d. columns. The injection volume was 0.5 µL. Analytes were detected at 254 nm. The retention times of analytes on each trap column maintained at 22 °C were compared to each other and those obtained from the isocratic separation of the same compounds on the 2.1 mm i.d. separation column used alone and kept at 70 °C.

Then, we examined the effect of the introduction of trap columns in the conventional direct injection configuration using gradient separation of iRT peptides, which was carried out on the trap-elute and the direct injection configuration separately. The trap and separation columns were maintained at 22 and 70 °C, respectively. To estimate the time that peptides spend on the trap columns, we also separated iRT peptides on the trap column used alone at 22 °C under the same conditions of gradient elution. Peptides were separated using a linear gradient method comprising 1-41% component B within 10 and 30 min followed by a fast increase to 80% component B as a 2-min column wash and finished by column equilibration at 1% component B for the time needed to reach stable back pressure before the next injection. The injection volume was 1 µL. The compared parameters were peak width at half height and retention time. The obtained results for the finally selected trap column were then confirmed on the LC-MS instrument under the same chromatographic conditions. For LC-MS experiments, Milli-Q water was replaced with LC-MS grade water. The results of LC-MS analyses were evaluated in Skyline v22.1.

The selection of the trap column suitable for the microbore 1.0 mm i.d. separation column was substantially simplified: the isocratic separations of small molecules were no longer performed since they had provided identical information to gradient separations of peptides for purposes of column comparison. For peptide separations, the only remaining gradient length was 30 min. The flow rate was reduced to 68 µL/min. The equilibration time before the next injection was prolonged. The iRT peptide mixture was diluted 4.4-fold to keep the injection volume constant in LC-UV experiments. In LC-MS experiments, it was additionally reduced to 0.2 µL because of increased overall MS signal intensity. Ion source parameters and ESI probe depth were adjusted due to the change in the flow rate, but the parameters of the mass analyzer remained the same.

We also examined the effect of the trap column temperature via the same approach involving iRT peptide separations. For the columns selected for LC-MS experiments, the aim was to find an optimum value providing maximum separation performance. For the columns that had demonstrated worse results – to evaluate their potential applicability at higher temperatures, even sacrificing the profitability of the entire trap-elute configuration. Besides selecting the trap columns and tuning their temperature, we also optimized the concentration

of the mobile phase acidifier and dimensions of the capillary connecting the trap and separation column. Each variable was tested one by one under other conditions kept constant. The settings providing the best peak widths were subsequently applied in LC-MS experiments.

4.2.3. Proof of hypothesis: LC-MS analysis of whole-cell proteome with integration of trap-elute setup

Ten micrograms of the whole-cell digest of the *F. tularensis* live vaccine strain were separated using direct injection on the narrow-bore 2.1 × 150 mm Acquity Premier CSH C_{18} column kept at 30 and 80 °C, and the trap-elute setup consisting of the trap 2.1 × 5 mm Acquity UPLC Protein BEH C_4 VanGuard Pre-column maintained at 35 °C and the mentioned separation column – at 80 °C. Mobile phase components were 0.05% formic acid in LC-MS grade water (component A) and 0.05% formic acid in LC-MS grade acetonitrile (component B). Peptides were eluted using a linear gradient running from 0.5 to 44.5% component B in 30 min. An isocratic hold at 0.5% component B was run first after the sample injection for durations of 0, 30, 60, 120, and 240 min before the gradient elution to mimic long analysis times common to exploratory bottom-up proteomic analyses. To suspend the elution of peptides during this isocratic in-column incubation, the mobile phase flow rate was set to decrease to 25 µL/min 30 min after injection within 1 min and to increase back 30 min before the gradient step (only in analyses with the isocratic steps of 120 and 240 min). The experiment was divided into parts each requiring about 18 hours of instrument time. A separate sample aliquot was dedicated for each part and was thawed right before analysis to ensure consistency of sample age (i.e., time after defrosting) between each run in the three data sets of analyses at 30, 80, and 35/80 °C (separation column temperature/trap column temperature).

The LC-MS data were searched using Byonic v3.5.0 against the *F. tularensis* subsp. *holarctica* protein database downloaded from UniProt (ID: UP000076142). A semi-tryptic cleavage was used with a maximum of 1 missed cleavage allowed. Mass tolerance was set at 7.5 ppm for precursors and at 10 ppm for fragments. Carbamidomethylation of Cys was set as a fixed modification. Oxidized Met, pyroGlu formation from N-terminal Glu and Gln, dehydrated Asp, and deamidation of Asn were set as dynamic modifications. Only spectra acquired during the gradient step were included in the data search. The results from the search were also used to compare the extent of non-enzymatic Asp-specific peptide cleavage. That is why semi-tryptic cleavage was used for the data search. Only PSMs identified with the two-dimensional FDR ≤ 1.0% were taken into consideration.

4.2.4. Application 1: Exploratory microflow LC-MS analysis of Jurkat cell proteome

The analysis of lysed and digested Jurkat cells was carried out using the optimized trap-elute configuration consisting of the 1.0 × 5 mm trap column custom-packed with Acquity UPLC Protein BEH C_4 and the microbore separation 1.0 × 150 mm Acquity Premier CSH C_{18} column maintained at 35 and 80 °C respectively. Analyses were also replicated using direct injection on the separation column kept at 30 and 80 °C. Unlike the previous section, separation was performed without the isocratic incubation step but using linear gradient methods lasting 30, 60, 120, and 240 min. They comprised 0.5-42.5% component B in 30- and 60-min analyses and

0.5-39.5% component B in 120- and 240- min analyses. The mobile phase components were the same as in the previous experiment. Two micrograms of peptides were separated within a 30-min gradient, 4 µg in 60 min, 10 µg in 120 min, and 20 µg within 240 min. The mobile phase flow rate was 50 µL/min and kept constant. The experiment was again divided into segments of similar required instrument time. The same sample management was applied.

For a comprehensive investigation of the effect of trap column installation on method sensitivity, only the 30-min gradient method was used. Injected masses were 50, 125, 300, 800, and 2000 ng for both configurations. Analyses at 30 °C were not performed. To eliminate a risk of carry-over that would increase the number of identified peptides in subsequent injections, we examined individual injection masses in ascending order with proper column wash after each injection. The trap-elute setup was tested first, followed by the direct injection configuration. Two identical sample aliquots were dedicated for both parts. The second aliquot was stored in a freezer at 80 °C until the measurement of trap-elute configuration was completed. The whole experiment was repeated with the reversed order of tested configurations using fresh sample aliquots to avoid potential bias caused by sample aging.

The LC−MS data were searched in Proteome Discoverer v2.3 using Byonic v3.5.0. After data recalibration using a rapid search against the human protein database downloaded from UniProt (ID: UP000005640), the spectra were thoroughly searched against the same protein database and its decoy form. The mass tolerance was set at 7.5 ppm for precursors and 20 ppm for fragments. Carbamidomethylation of Cys was set as a fixed modification. Full-tryptic specificity was used with a maximum of two missed cleavages allowed. Oxidized Met and protein N-terminal acetylation were set as dynamic modifications for a conventional LC−MS data search. For the search that considered thermally induced Asp-specific cleavage and modifications, the trypsin specificity was changed to semi-specific. Besides the modifications involved in the conventional search, pyroGlu formation at the N-terminal Glu and Gln, dehydration of Asp, and ammonia loss from Asn were added as dynamic modifications. Only PSMs identified with the two-dimensional FDR ≤ 1% were taken into consideration.

4.2.5. Application 2: Multi-attribute LC-MS method for characterization of therapeutic proteins

Ten micrograms of digest of trastuzumab, bevacizumab, and aflibercept were separated using a trap-elute setup consisting of 2.1 × 5 mm Acquity UPLC Protein BEH C_4 and the narrow-bore separation 2.1 × 150 mm Acquity Premier CSH C_{18} column maintained at 35 and 80 °C respectively, and direct injection on the same separation column kept at 30 and 80 °C. The separation method began with a 1-min isocratic hold at 0.5% component B for elution of compounds of non-peptide structure, followed by 110-min gradient elution. The flow was diverted to waste during the first 1.3 min to prevent ion source contamination. A linear gradient method was developed for each drug based on the retention time of the last eluted peptide in the digest. The upper value of the component B fraction was set so that this peptide eluted no later than 5 min before the end of the gradient. For trastuzumab, this value was 28.5% component B, for bevacizumab – 30.5%, for aflibercept – 27.5%. For analyses performed on the separation column maintained at 30 °C, both the initial and the final value of the component B fraction in the method were increased by 1% to minimize differences from the retention time of peptides observed in analyses at 80 °C.

The LC-MS data were searched using MSFragger integrated within Skyline v22.1 against the FASTA sequences of the proteins enriched with common contaminants. The cut-off score was set at 0.95. Trypsin cleavage was set as semi-specific, with a maximum of 2 missed cleavages allowed. Only variable modifications were included as follows: ammonia loss from Asn, dehydration of Asp, oxidation of Met, and pyroGlu formation from N-terminal Glu and Gln. Possible precursor charges were 2, 3, 4, and 5. Monoisotopic peaks were included in a count of 3 with mass tolerance set at 8 ppm. The mass tolerance for fragments was set at 18 ppm. Only MS1 scans in an interval of 8 min around the time of MS/MS identification time were filtered.

5. RESULTS AND DISCUSSION

5.1. Trap Column Selection and Optimization of Analytical Conditions

The trap-elute setup development began with a 2.1 mm i.d. column format because of greater robustness and fast responsiveness. The first candidate trap column was a 2.1 × 30 mm Accucore 150-C_4 column. We performed isocratic elution of the small-molecule standard, which consists of uracil, acetophenone, toluene, and naphthalene in balanced concentrations. Uracil was used for the estimation of void time as it is almost not retained in the columns involved in the study. We compared retention time and retention factors of the other 3 analytes obtained from the trap and the separation column separately (Figure 3):

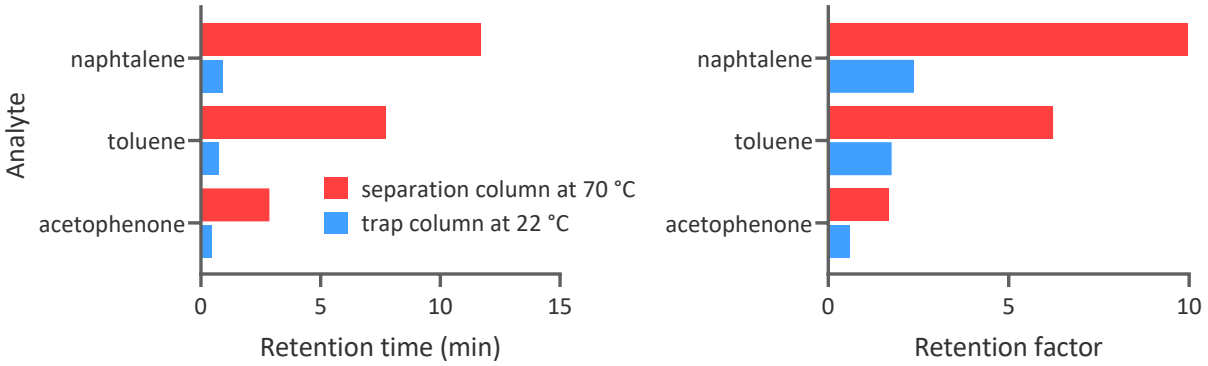

Figure 3: Retention time and retention factors of small-molecule analytes obtained from the trap 2.1 × 30 mm Accucore 150-C_4 column (22 °C) and the separation 2.1 × 150 mm Acquity Premier CSH C_{18} column (70 °C) under the conditions of isocratic elution at 40% component B. The standard deviation of replicates is not shown since it does not exceed 0.5% in all analyses. The further figures in the text that do not illustrate any standard deviation follow the same rule.

Greater retention factors and retention time of peptides on the separation column proved the desired difference in the retentivity of both columns. Therefore, we proceeded to the gradient separation of iRT peptides using direct injection on the separation column and the trap-elute setup with this trap column.

Unfortunately, we noticed significant peak broadening associated with the installation of the trap column, accompanied by a shift in retention time (Figure 4):

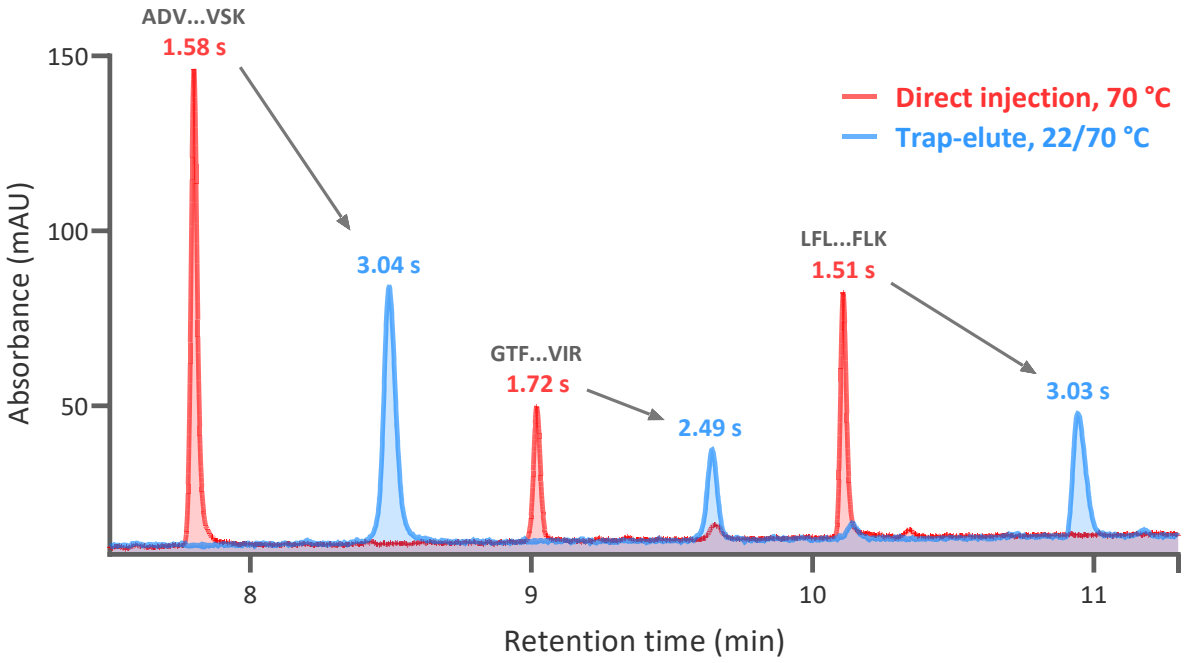

Figure 4: Overlaid chromatograms of the 10-min gradient separation of iRT peptides using direct injection on the separation 2.1 × 150 mm Acquity Premier CSH C_{18} column (70 °C) and the trap-elute setup with the trap 2.1 × 30 mm Accucore 150-C_4 column installed upstream (22/70 °C). The peak widths at half height are illustrated under peptide sequences with the corresponding coloring. Arrows demonstrate the shift in retention time and peak broadening. The last three eluted peptides are only shown to avoid peaks of different peptides overlapping in analyses with and without the trap column.

Additionally, we compared the retention time of peptides obtained from the trap-elute setup and the trap column installed alone and calculated the portion of total in-column residence time that peptides spend being retained in the trap column (Figure 5):

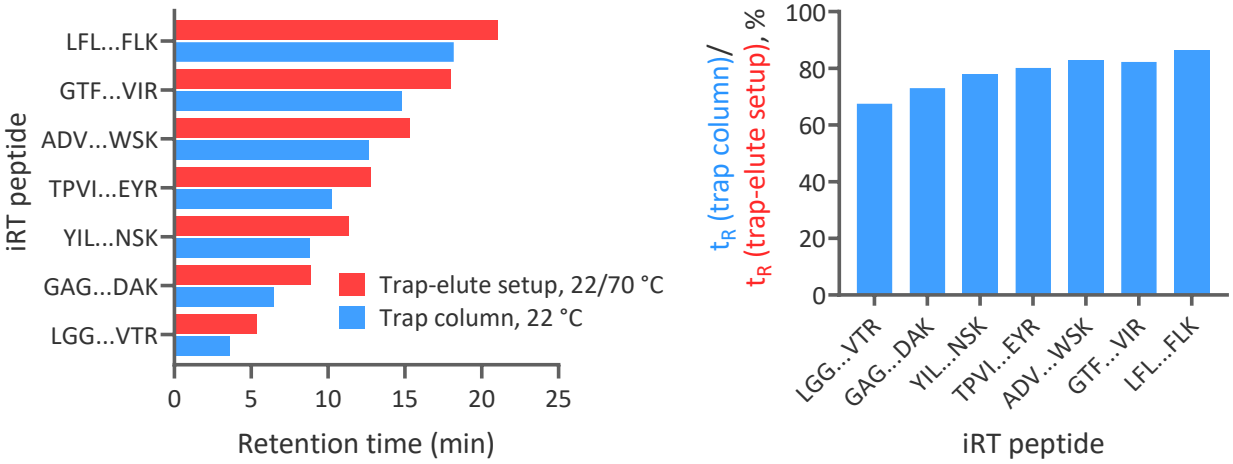

Figure 5: Retention time (t_R) of iRT peptides obtained from the 30-min gradient separation using the trap-elute setup (22/70 °C) and the trap column (22 °C) installed alone. The right figure illustrates the portion of total in-column residence time that peptides spend being retained in the trap column if it is included in the setup.

The calculation demonstrates that peptides spend the major portion of analysis time in the trap column maintained at the safer temperature of 22 °C. This portion increases with the gradient time extension and hydrophobicity of peptides. As we had previously hypothesized, it could reduce unwanted artifact formation. However, the trap column installation also worsened the peak shape of peptides. This would result in worse separation performance and impair the method sensitivity, one of the critical method characteristics. The aim to preserve the method sensitivity becomes more critical because, in case of worsened sensitivity, the potential decrease in the number or quantity of identified artifacts would not result from the concept effectiveness but from simple peak broadening, leading either to intensified competition with high-abundant intact peptides or even to the drop of artifact peak intensity under the limit of detection. The artifacts would be naturally discriminated in this case since they are typically present in minor concentrations and are especially vulnerable to a drop in separation performance. In that case, the analysis of all low-abundant peptide modifications would be compromised as peak broadening affects all peptides regardless of their origin.

We assumed that the cause of the observed peak broadening is a too-small difference in retentivity of the trap and separation column, which means that peptides leave the trap column too late, with the mobile phase that is already too strong to enable efficient refocusing at the head of the separation column. As the preservation of the separation performance was the priority, we decided to shorten the time that peptides spent in the trap column. There were two options: a weaker stationary phase or a shorter trap column. Alternatively, there was an option to select a more retentive separation column. The CSH C_{18} particle chemistry is indeed considered one of the least retentive options [10] due to the placement of the positively charged moieties on the particle surface [68]. It understandably complicates the trap column selection. On the other hand, only this particle chemistry possesses unique features in terms of separation of peptides in a low-ionic-strength mobile phase and reduced secondary interactions. That is why we avoided the substitution of the advantageous separation column but proceeded to the change in the trap column. We were not aware of any commercially available trap columns with less retentive stationary phase that would have fitted our needs. Therefore, we tried out a shorter 2.1 × 5 mm Acquity UPLC Protein BEH C_4 VanGuard trap column with a constant stationary phase ligand. This column also has wider particle pores, potentially possessing lower retentivity due to reduced surface area. The isocratic separation of small-molecule analytes showed the expected drop in retentivity (Figure 6):

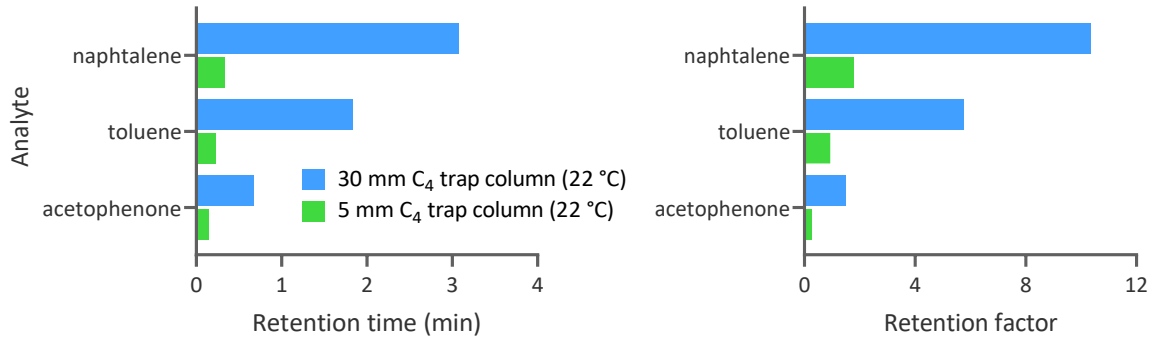

Figure 6: Retention time and retention factors of small-molecule analytes obtained from the two trap columns (2.1 × 5 mm Acquity UPLC Protein BEH C_4 VanGuard and 2.1 × 30 mm Accucore 150-C_4 column) under the conditions of isocratic elution at 30% component B.

Also, there was only minor peak broadening and the shift in retention time of iRT peptides after the installation of the trap column compared to the results from the 30-mm trap column (Figure 7):

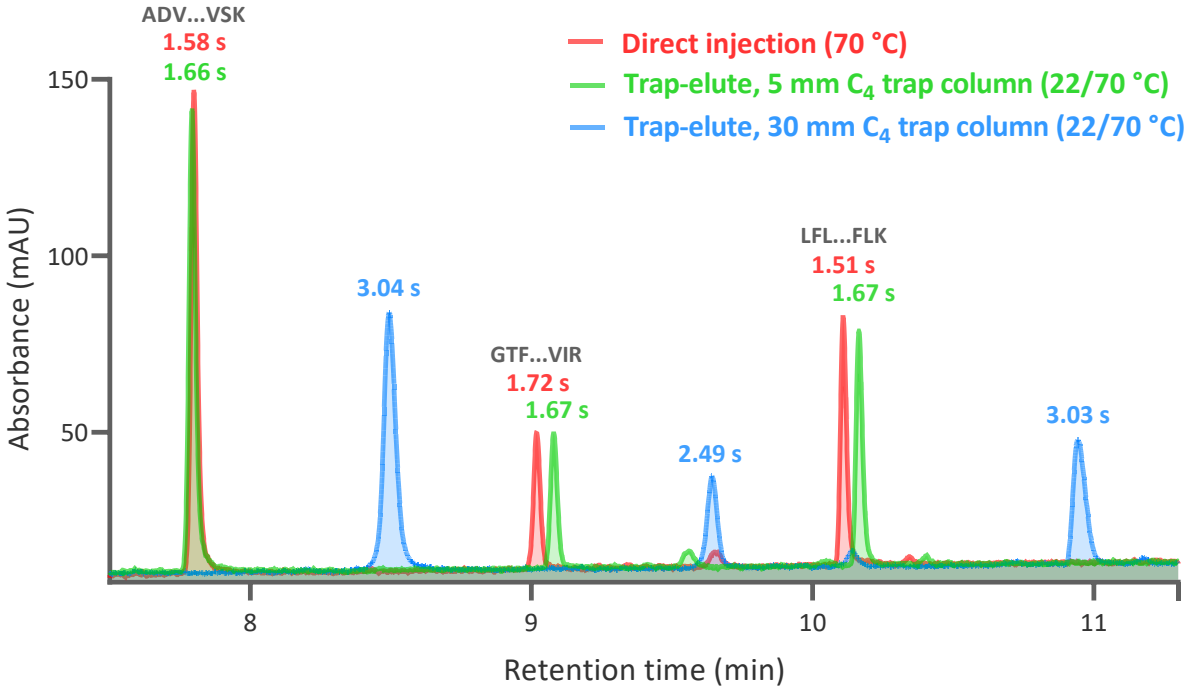

Figure 7: Overlaid chromatograms of the 10-min gradient separation of iRT peptides using direct injection on the separation 2.1 × 150 mm Acquity Premier CSH C_{18} column (70 °C) and the trap-elute setup with the trap 2.1 × 5 mm Acquity UPLC Protein BEH C_4 VanGuard or 2.1 × 30 mm Accucore 150-C_4 column installed upstream (22/70 °C). The peptide peak widths at half height are illustrated above with the corresponding coloring. The last three eluted peptides are shown.

Expectedly, the portion of the analysis time spent by peptides in the trap column decreased proportionally (Figure 8):

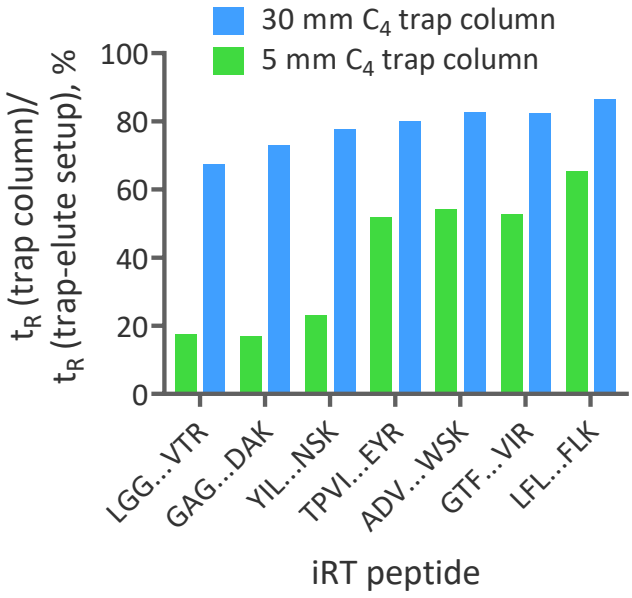

Figure 8: The portion of the total in-column residence time that iRT peptides spend being retained in the trap 2.1 × 5 mm Acquity UPLC Protein BEH C_4 VanGuard or 2.1 × 30 mm Accucore 150-C_4 column (22 °C) while included in the trap-elute setup. Data from the 30-min separation are shown.

We also noticed weak retention of the 3 most hydrophilic peptides, which might predict poor improvement of the modification extent of hydrophilic peptides in general. However, the less hydrophobic the peptide, the less time it spends on the heated column before elution. Thus, the modification extent of

quickly eluting peptides is expected to be smaller based on the general dependency of modification extent on the in-column residence time. That is why we assumed that weak retention of hydrophilic peptides in the trap column would not compromise the trap-elute setup efficiency.

Based on the experiments with the two trap columns, we established several relationships that drove the following attempts in the trap column selection: the more retentive/lengthy the trap column, the more time peptides spend in the relatively safe environment of the trap column instead of being retained in the heated separation column, but the less effective is the further refocusing at the head of the separation column and the worse the resulting peak shape. The shift in the retention time may serve as an additional marker of the incorrect trap column selection. The less retentive/shorter the trap column, the less it impairs the separation performance, but the smaller the benefit in terms of prevention of peptide modification. The second examined trap column was considered the least retentive option, which fits the requirement to preserve the separation performance but might not be that efficient in the prevention of artifact formation. Therefore, we sought to find a compromise option between the two tested retentivity extremities, which resulted in an examination of the next two trap columns with expected greater retentivity: 2.1 × 10 mm Accucore 150-C_4 and 2.1 × 5 mm Acquity UPLC BEH C_8 VanGuard Pre-column. The first one represents the already exploited way to tune the trap column retentivity by the change in the column length. The second column has the same column length and particle chemistry as the Acquity UPLC Protein BEH C_4 VanGuard Pre-column but is not explicitly dedicated to protein separations. It has the more retentive C_8 stationary phase ligand and smaller particle pores.

Briefly, these two trap columns demonstrated peptide retention time laying between those from the initially tested columns, but the peak shape was again worsened similarly to the case of the 2.1 × 30 mm Accucore 150-C_4 column (*see Figure S2 in Supp. Materials*). Although the average peak width shows a large standard deviation because of the non-equal peak width of different peptides, it does not make this parameter unconvincing since all peptide peak shapes behave similarly when broadened by the factor influencing all peptides. As the peak shape was the priority, the finally chosen trap column was the 2.1 × 5 mm Acquity UPLC Protein BEH C_4 VanGuard Pre-column, being the only trap column that demonstrated a negligible effect on the separation performance.

Along with attempts to find the optimum conditions via changes in the trap column dimensions and stationary phase, we also tried to adjust the column temperature regime to reach a balanced difference in peptide retention on the trap and separation column. For most analytes, it is valid that the higher the column temperature, the shorter the retention time. Applied to the optimization of the trap-elute setup, there was an option either to elevate the trap column temperature to lower its retentivity or to reduce the separation column temperature to increase its retentivity. We speculate that for many of the examined trap columns, it was feasible to find the temperature regime that would make the installation of the trap column imperceptible, but for most trap columns, it would result in the temperature conditions barely profitable for the prevention of artifact formation and full exploitation of the high column temperature. In other words, we could try to elevate the trap column temperature to mitigate the peak shape worsening, but it would result in a smaller profit for peptide modification. Analogously, we could lower the separation column temperature, but it

would only partially enhance the separation performance compared to LC at traditional temperatures. Therefore, both described measures were undesired and applied to the minimum required extent only when necessary.

The utilization of the trap 2.1 × 5 mm Acquity UPLC Protein BEH C_4 VanGuard Pre-column was possible under the initial temperature regime, i.e., 22/70 °C. However, to evaluate the potential applicability of other trap columns (2.1 × 10 and 2.1 × 30 mm Accucore C_4-150 columns), we repeated gradient separations of iRT peptides under alternative column temperature regimes: 22/50 °C and 50/50 °C (Figure 9):

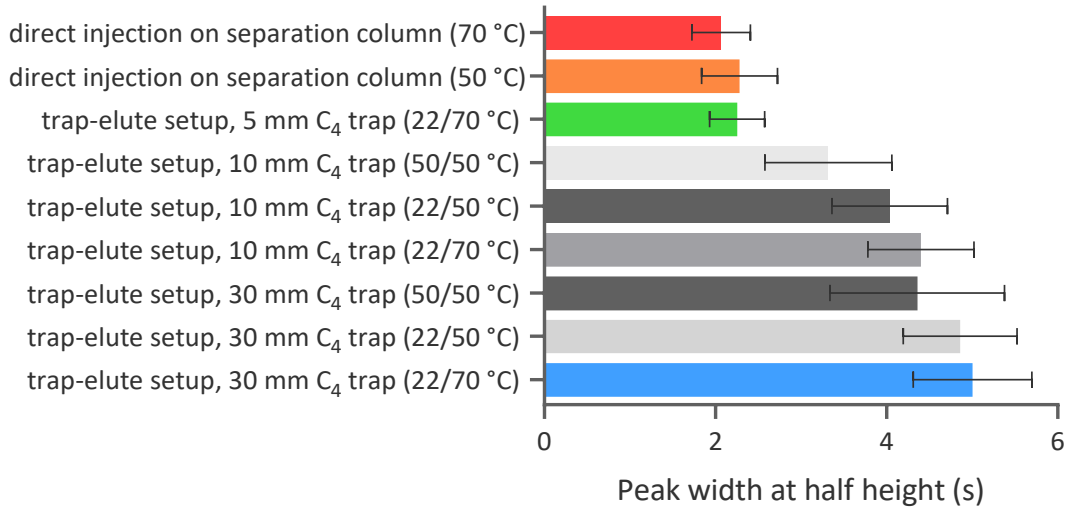

Figure 9: Average peak widths of iRT peptides obtained under different temperature regimes (trap column temperature/separation column temperature) and using 3 different C_4 trap columns. The data from the 30-min gradient separation are shown.

The first regime (22/50 °C) remains potentially profitable in terms of formed artifacts and exploits the lower but still elevated column temperature. However, the second regime (50/50 °C) is not advantageous at all. It was used only to determine if it is possible to couple a trap column to the given separation column, at least under unrestricted temperature conditions. The experiment revealed only a minor effect of lowering the separation column temperature from 70 to 50 °C on average peak width when this column is included in the trap-elute setup. When the temperature of both columns was changed towards the equal value of 50 °C, it had a more significant effect. But still, the peak widths before and after the trap column installation were too far from each other even under the temperature regime that is completely useless for the project's purpose. Hence, we conclude that the only applicable trap column (even if the temperature regime is changeable) for coupling with the separation 2.1 × 150 mm Acquity Premier CSH C_{18} among the 4 tested trap columns is 2.1 × 5 mm Acquity UPLC Protein BEH C_4 VanGuard Pre-column. However, when the trap-elute setup was later transferred to the LC-MS instrument and the separation column temperature was changed from 70 to 80 °C, we observed slight peak broadening likely caused by the reduced difference in the column retentivities. This eventually required elevation of the trap column temperature from the ambient 22 to 35 °C to get back the desired peak shape.

After the trap column was selected for the narrow-bore 2.1 mm i.d. separation column, we proceeded to the 1.0 mm i.d. one. The first tested trap column was the column previously

selected for the 2.1 mm i.d. trap-elute setup. The separation column temperature was set at 80 °C from the very beginning – in contrast to the trap column selection for the 2.1 mm i.d. separation column, where we started with 70 °C and then switched it to 80 °C during setup transfer to the LC-MS instrument. This is because the intention to use it at 80 °C in the LC-MS experiments was already clear in the beginning.

Unfortunately, the difference in i.d. between the trap and separation column resulted in significant peak broadening. The trap column of 2.1 mm i.d. has a 4.41-fold larger volume than a hypothetical 1.0 mm i.d. trap column of the same length. If the flow rate is constant, the mobile phase passes this broader trap column for a 4.41-fold longer time. We would expect the same increase in passage time if we compared two trap columns of the same i.d. but with a 4.41-fold difference in length. This was particularly the case of the 2.1 × 5 and 2.1 × 30 mm C_4 trap columns that we had tested at the beginning for the 2.1 mm i.d. separation column, where we observed peak broadening in results from the lengthy one. Here, we again observed broadened peaks using a broader trap column, similarly to the experiments with a longer trap column. That is how we explain the nature of peak broadening resulting from the inappropriate choice of trap column i.d. Even when this 2.1 mm i.d. trap column was heated to the maximum tolerated temperature of 45 °C, the peak width increase was too far from the previous results for the 2.1 mm i.d. trap-elute setup. This is why the i.d. of the next candidate trap columns for the 1.0 mm i.d. separation column was restricted to 1.0 mm, even though the assortment of trap columns with the C_4 stationary phase ligand and dimensions of 5 × 1.0 mm was limited. We examined two commercially available EXP trap columns that fulfill the mentioned conditions, but the observed peak width increase led us to purchase the trap column with dimensions of 5 × 1.0 mm custom-packed with the stationary phase particles of the 2.1 × 5 mm Acquity UPLC Protein BEH C_4 VanGuard Pre-column. Only this trap column provided the effect on the peak shape comparable to that obtained from the trap column coupled with the 2.1 mm i.d. separation column (Figure 10). However, this trap column must be heated to 35 °C as well as in the 2.1 mm i.d. trap-elute setup. Thus, the setups of both column diameters have a unified temperature regime of 35/80 °C.

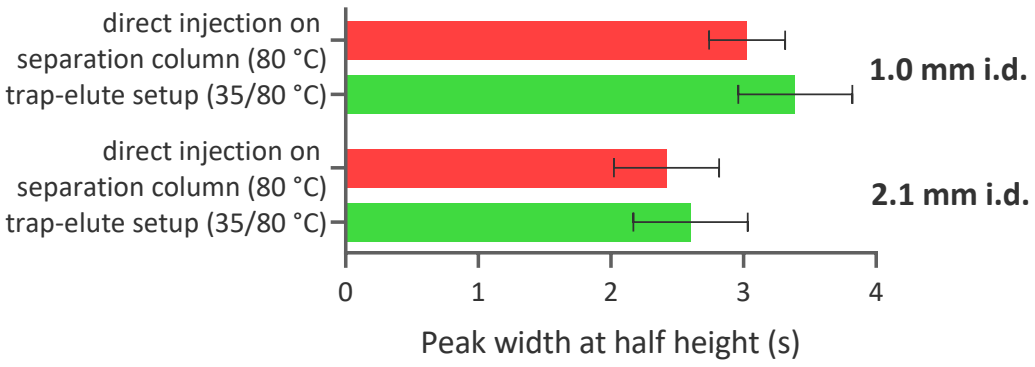

Figure 10: Average peak width of iRT peptides analyzed using the trap-elute setup and the direct injection configuration of both column diameters. The data from the 30-min gradient separation performed on the LC-MS instrument are shown.

For both trap-elute setups, we also examined the effect of the capillary connecting the trap and separation column on the peptide peak width. This capillary must be placed in the

thermostat that heats the separation column so that the mobile phase outflowing from the trap column is preheated to the temperature of the separation column before it enters the column. It must have sufficient volume so that the time of mobile phase passage through the capillary is enough for complete preheating. Preferably, the capillary should be made of well-thermally conductive material and placed close to the heated parts of a thermostat. Also, the higher the ratio of the capillary external surface area to its internal volume, the more efficient the preheating. All these measures enable the cooling of the separation column to be avoided by the inflowing mobile phase, which would create a thermal gradient along the column, resulting in peak distortions [104]. On the other hand, the large volume of the capillary would broaden peaks due to diffusion, even though this consequence would be partially mitigated by downstream refocusing at the head of the separation column.

These relationships led to the assumption that inappropriately selected capillary may be the cause of the observed peak width increase due to the trap column installation – either because of incomplete mobile phase preheating or excessive diffusion. This is why we compared the peak width of iRT peptides obtained from the separation using the developed trap-elute setups of both column diameters assembled with different connecting capillaries, including the 0.1 × 380 mm capillary with the active preheater initially installed and used on the LC-MS instrument (Figure 11):

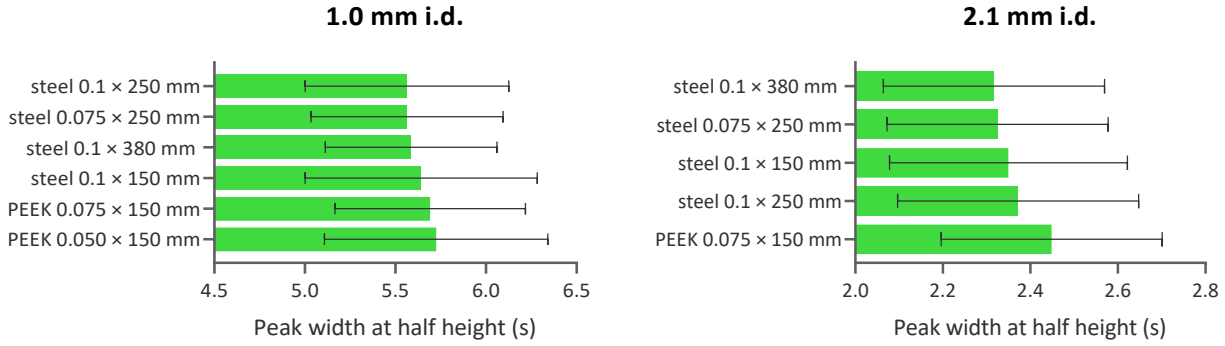

Figure 11: Average peak width of iRT peptides obtained using the 2.1 and 1.0 mm i.d. trap-elute setups (35/80 °C) assembled with different capillaries. As the experiment was carried out on the LC-UV instrument incompatible with active preheaters from Thermo Fisher Scientific, the active preheater was not connected and worked as a passive preheater. The data from the 30-min separation are shown.

For both column diameters, the selection of the connecting capillary was only shown to be a minor contributing factor. The difference in the average peak width between the best and the worst capillary did not exceed 3%, except for the smallest 0.075 × 150 mm nanoViper PEEK capillary connecting the 2.1 mm i.d. column setup that broadened the peaks by 5.7% on average. Therefore, we conclude that any of the listed stainless-steel capillaries can be effectively used, provided that the major portion of the capillary is placed in the separation column thermostat. Due to the higher flow rate used for the operation of the 2.1 mm i.d. setup, it is more vulnerable to the use of the smallest capillaries. This is because the time of mobile phase passage through the capillary is 4.4 times shorter than if it was operated using the flow rate of 68 µL/min set for the 1.0 mm i.d. setup. Consequently, non-steel capillaries (with worse thermal conductivity) of dimensions as small as the mentioned 0.075 × 150 mm should be avoided. Regarding the steel capillaries, we decided to use the 0.1 × 380 mm capillary with the

active preheater from Thermo Fisher Scientific in the following LC-MS experiments since it is the only capillary enabling active preheating and is lengthy enough to easily connect the columns placed in two separate thermostats.

Based on the previous findings regarding the dependence of peptide retention on CSH and BEH columns on mobile phase acidity, it was considered a potential tool for increasing the difference in peptide retention on the used BEH trap and CSH separation columns. Therefore, we compared the peak width of iRT peptides obtained from the separation using setups of both column i.d. using mobile phase acidified with 0.05% and 0.1% formic acid (*see Figure S3 in Supp. Materials*). Expectedly, the lower concentration of formic acid provided better peak shapes. 0.05% formic acid was then used in LC-MS analyses with both trap-elute setups, consistently with the LC-UV experiments. The initial LC-UV experiments were performed with 0.05% formic acid only because of the UV detector cut-off. At the time these experiments were carried out, the effect of the formic acid concentration on the peptide retention in these stationary phases had not been described yet. That is why this factor was not considered during the design of the LC-UV experiments.

5.2. Proof of Hypothesis: LC-MS Analysis of Whole-Cell Proteome with Integration of Trap-Elute Setup

To prove the hypothesis that the shortening of the in-column residence time by installation of a less retentive trap column upstream reduces artifact formation, we designed an experiment similar to that performed by *Lenčo et al.* in a recent study [3]. The experiment simulates a typical single-shot long-gradient LC-MS analysis of a complex sample. The whole-cell bacterial digest was analyzed using the 2.1 mm i.d. trap-elute setup (35/80 °C) and direct injection on the 2.1 mm i.d. separation column maintained at 80 and 30 °C. The high-temperature analysis served as the illustration of the number of modified peptides that are generated at elevated column temperature if no preventative measures are applied. At the same time, it shows how many peptides from the given sample can be identified in total by the method exploiting direct injection on the heated separation column. This can be used as a straightforward measure of method productivity. Using the number of identified peptides, we can compare the separation performance of the proposed method to the conventional approach. The low-temperature analysis demonstrates the smaller number of peptides identified using the method that runs at a near-to-ambient temperature. Then, it provides the number of identified artifacts that originate mainly from the sample preparation/storage and *in vivo* modification. As the column temperature can be barely lowered more due to the generated back pressure, the number of artifacts generated during the separation at 30 °C can be considered the lowest achievable. We assume that this number is negligible compared to the number of artifacts generated before LC-MS analysis. Thus, the number of identified artifacts obtained from the separation at the low temperature represents the target value for the trap-elute setup development.

A long shallow gradient was substituted with an isocratic hold at 0.5% component B of ascending duration, followed by steep 30-min gradient elution. The isocratic step at this low mobile phase strength does not allow most peptides to leave the trap column in the

experiment with the trap-elute setup (or the head of the separation column in the experiment with the direct injection configuration) earlier than the gradient starts. Hence, this hold serves as an in-column incubation step. We expected that some number of peptides would elute and reach the MS detector during this step. These peptides would be "lost" since the data evaluation involved only peptides eluted during the gradient step. To prevent premature peptide elution, we might have turned off the mobile phase flow shortly after the injection. However, the system would be thus left with a flow rate of zero, which was considered undesirable. We reduced the flow rate during the incubation step as a compromise solution.

The experiment was aimed at the modification reactions strongly dependent on column temperature and the analysis time in the mentioned study by *Lenčo et al.* [3]. We compared the relative abundance of modified peptides among all identified peptides after in-column incubations of different lengths under the three analytical conditions (Figure 12):

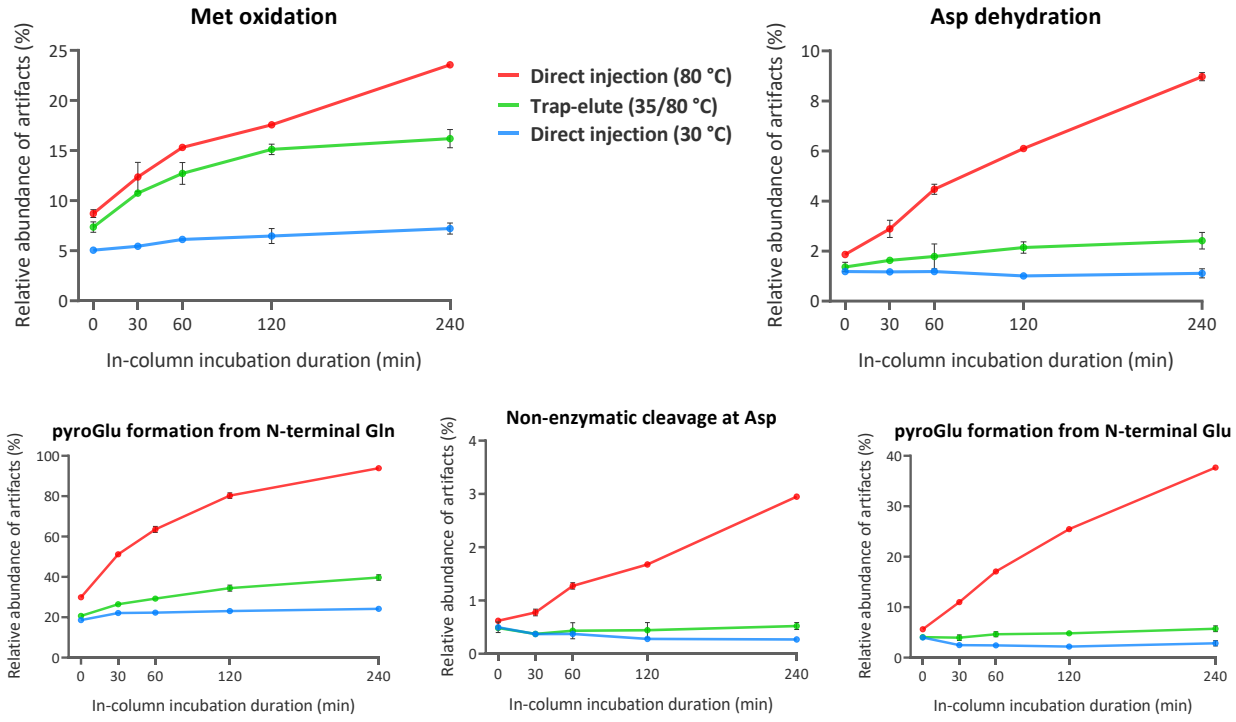

Figure 12: Relative abundances of temperature-related artifacts among all peptides identified in analyses of a whole-cell digest of *F. tularensis* live vaccine strain performed using the 2.1 mm i.d. trap-elute setup (35/80 °C) and direct injection on the 2.1 mm i.d. separation column maintained at 30 and 80 °C. Post-injection in-column incubation under isocratic conditions at 0.5% component B is followed by 30-min gradient elution. Standard deviations smaller than the size of data symbols are not shown.

The relative abundance was calculated for distinct modifications as a number of peptides containing the modified amino acid residue divided by the summed number of peptides containing both the modified and unmodified amino acid residue. For the N-terminal pyroGlu formation, it was divided by the summed number of peptides that only start either with Glu or Gln at the N-terminus regardless of the identified peptide form. For Asp-specific non-enzymatic cleavage, it was calculated separately as a number of peptides cleaved at the C- or

N-terminus of Asp by non-tryptic hydrolysis both divided by the total number of peptides containing Asp. The figure demonstrates that the trap-elute setup indeed managed to reduce the relative abundance of traced artifacts. In line with previous findings of *Lenčo et al.*, the number of artifacts increases with the column temperature and the gradient time. The profit from trap column installation increases towards longer incubation times, making it especially advantageous for long analyses. This is supported by the previous observation that the portion of the total in-column residence time that peptides spend in the trap column increases with the gradient time. For Asp dehydration and pyroGlu formation, the artifact abundance almost dropped to that observed in the low-temperature analysis, which provides the minimum modification extent ("baseline"). The same trend was observed for Asp-specific non-enzymatic cleavage, especially in the abundance of C-terminal cleavage that more strongly correlates with the column temperature and the in-column residence time. We speculate that it is likely caused by the slower kinetics of these reactions, meaning that these artifacts require longer in-column residence time or higher temperature to be formed. In other words, peptides elute from the trap column too late to undergo a "full-scale" modification process and form artifacts in quantity sufficient to reach a detection limit before they leave the separation column. This may explain why the decrease in the abundance of these artifacts is more significant than in the case of Met oxidation. Despite the differences in the results for distinct modifications, we concluded that the hypothesis was confirmed and proceeded to the test applications.

5.3. Application 1: Exploratory Microflow LC-MS Analysis of Jurkat Cell Proteome

The design of the previous experiment enabled us to test the study hypothesis reliably. However, the method sensitivity and separation performance described via the number of identified peptides could not have been evaluated because of the bias resulting from the prepended isocratic step and the data evaluation approach limited to the peptides eluted during the short gradient step. That is why the real-life gradient method was necessary. Furthermore, by this concept of the prepended incubation, the portion of in-column residence time spent by peptides in the trap column is artificially increased in comparison to the time that peptides would have spent in the trap column in a real-gradient analysis. Due to this, we expected less significant improvement in the artifact abundance in the real gradient analyses. To better simulate typical exploratory LC-MS analyses, the microflow 1.0 mm i.d. trap-elute setup was used in contrast to the previous experiment. The prokaryotic bacterial sample was replaced by the eukaryotic human cell line digest to increase sample complexity and, consequently, statistical confidence of results.

First, we again compared the relative abundance of artifacts in the same manner (Figure 13):

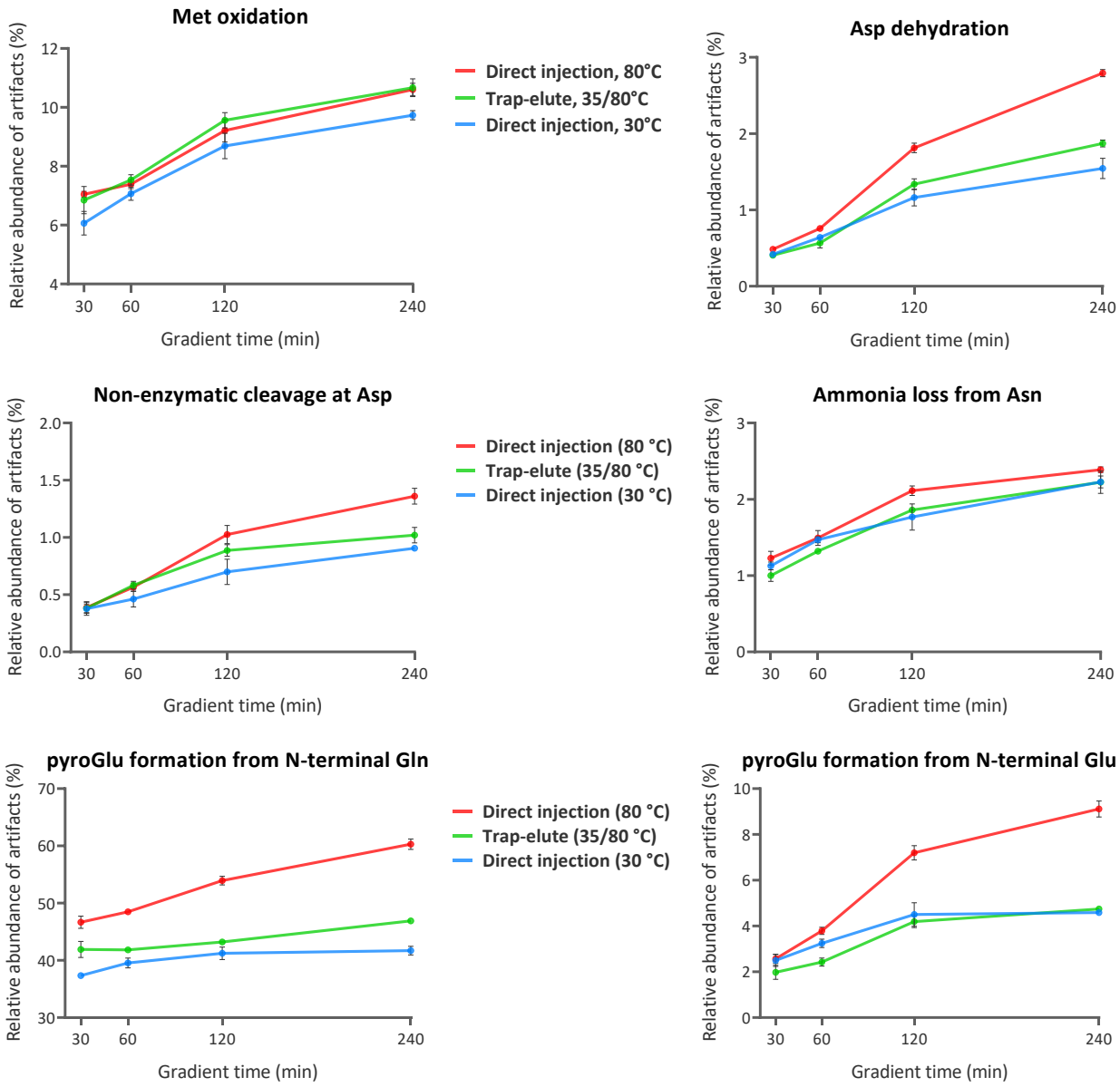

Figure 13: Relative abundances of temperature-related artifacts among all peptides identified in analyses of the Jurkat cell line digest performed using the 1.0 mm i.d. trap-elute setup (35/80 °C) and direct injection on the 1.0 mm i.d. separation column maintained at 30 and 80 °C. Standard deviations smaller than the size of data symbols are not shown.

For Asp dehydration, pyroGlu formation, and Asp-specific non-enzymatic cleavage, the trap-elute setup preserved the capability to significantly reduce the relative abundance of identified artifacts even under the conditions of the actual gradient method. As expected, the decrease is slightly smaller than in the previous experiment. However, the trap column can still prevent the modification of at least 50% of peptides (up to the quantity sufficient for artifact detection) containing Asp or N-terminal Glu/Gln that otherwise would be modified if the high column temperature was applied without any preventative measures. On the other hand, there was no significant improvement in the extent of Met oxidation if the abundances of

identified artifacts were compared. We hypothesize that it may be again caused by the fast reaction kinetics. Likely, the portion of total in-column residence time that peptides spend in the separation column is still big enough to form these artifacts in the quantity needed for detection. Therefore, the only way to prevent their excessive formation would be to increase the peptide retention on the trap column. Unfortunately, this had been previously shown to be an unacceptable measure because of the rising peak broadening. The poor improvement in the number of peptides with oxidized Met led us to start also comparing the artifact quantities in the following test application, along with the traditional approach involving the number of identifications.

In contrast to the previous experiment, the peptides with deaminated Asn (ammonia loss) were also considered. In all subsequent experiments, this modification was considered regularly. We observed a similar dependency of the artifact abundance on the column temperature, analysis time, and the presence of the trap column in the configuration, even though the correlation between the modification extent and the column temperature is not as significant as for other modifications.

The next compared method characteristics were sensitivity and separation performance. We considered the number of identified peptides the most convenient means for the comparison of the trap-elute setup to the direct injection, provided that the only variables are the separation column temperature and the presence of the trap column in the configuration. However, during data evaluation, we realized that the total number of identifications increases with column temperature not only because of the effect of temperature on the separation performance but also because of the increased number of artifacts. The latter increases the total number of identifications but does not mean improved separation performance or method sensitivity (both influencing the method productivity) as the peak shape of intact "parent" peptides of interest remains constant. The quantity of intact peptides may decrease due to artifact formation, but it also does not indicate any changes in separation performance. Although modified peptides increase the total number of identified peptides, they only duplicate the sequences of intact peptides. They do not bring any additional biological information, which does not make the method more productive. That is why a comparison of the productivity of two methods that provide the same peak shape but generate different numbers of artifacts would be biased towards the ostensibly "better" method generating more artifacts. Applied to the comparison of the trap-elute setup and the direct injection, even if the actual separation performances were equal, we would observe a higher total number of identifications in the results from the direct injection due to a greater number of artifacts. This is valid if the data search parameters include thermal modifications.

On the other hand, if only intact peptides with an exception for Met oxidation were considered in data evaluation (see the conventional data search approach in Methods) in the effort to perform unbiased comparison, it would lead to the opposite result. When the less artifact is formed, the less intact peptide quantity is "consumed". As the trap-elute setup protects peptides from modification and helps to maintain the intact peptide quantity at the initial level, we would observe more identified intact peptides in the analysis using the trap-elute setup compared to the direct injection configuration with a heated separation column. Also, a certain portion of modified peptides eluting from the heated separation column no longer have an unmodified counterpart because it has been completely modified. Therefore,

if the conventional data search strategy was applied, the sequence segments represented only by modified peptides would not be covered.

To conclude, the comparison would be biased anyway, no matter which data search strategy is used. Stimulated by this fact, a hybrid means for method comparison was introduced. The data search strategy involved both modified and intact peptides of unrestricted cleavage specificity, but only one peptide per sequence segment was counted in the identification number used in the comparison. All the modified peptides that duplicate the sequence of an already found intact peptide were removed, so only unique peptide sequences remained. Thus, there is no increase in the number of identifications caused by the clusters of modified peptides that otherwise would be misinterpreted as a sign of improved method productivity. This eliminates the bias originating from the comparison of data searched using the parameters considering thermal modifications. On the other hand, this type of search still enables coverage of a certain protein sequence, even if this sequence is represented only by a modified peptide. In other words, this hybrid search strategy is not blind for modified peptides and still counts the peptides present only in the modified form but does not indicate ostensibly higher method productivity when a dataset contains clusters of modified peptides as sequence duplicities. This number of unique peptide sequences was used for an unbiased comparison of separation performance (Figure 14):

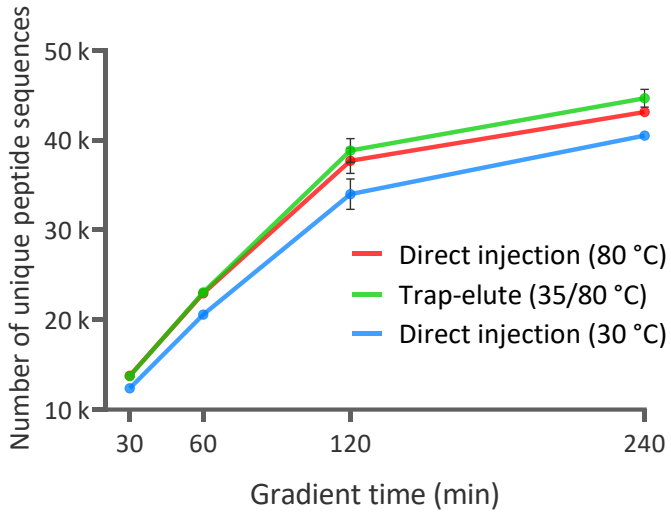

Figure 14: Number of unique peptide sequences identified in analyses of the Jurkat cell line digest performed using the 1.0 mm i.d. trap-elute setup (35/80 °C) and direct injection on the 1.0 mm i.d. separation column maintained at 30 and 80 °C. Standard deviations smaller than the size of data symbols are not shown.

In line with the previous findings, a larger number of peptides was identified in the analyses using the separation column kept at 80 °C. However, the relative increase in the number of identifications normalized to the low-temperature analysis starts to decrease from 10.9% in the 120-min analysis to 6.5% in the-240 min analysis, likely because of extensive artifact formation. The trap-elute setup provided the same number of identifications in 30- and 60-min analyses as the high-temperature analysis using direct injection. For 120- and 240-min runs, the installation of the trap column even increased the number of identified peptides compared to the analyses on the separation column kept at 80 °C by 3.1 and 3.6%, respectively. We trust that it is likely because the trap-elute setup helps to reduce the drop in the intact peptide peak intensity caused by artifact formation. Consequently, the peak intensity of this protected intact peptide will less likely drop under the intensity threshold of the MS/MS fragmentation trigger. Hence, the trap-elute setup demonstrated comparable productivity

resulting from the preserved separation performance and even showed the potential to prevent losses in identifications that normally occur in long gradient analyses using a heated separation column. We also extracted the numbers of modified peptides that duplicate the sequences of intact peptides and the numbers of peptides present in the datasets only in the modified form (Figure 15):

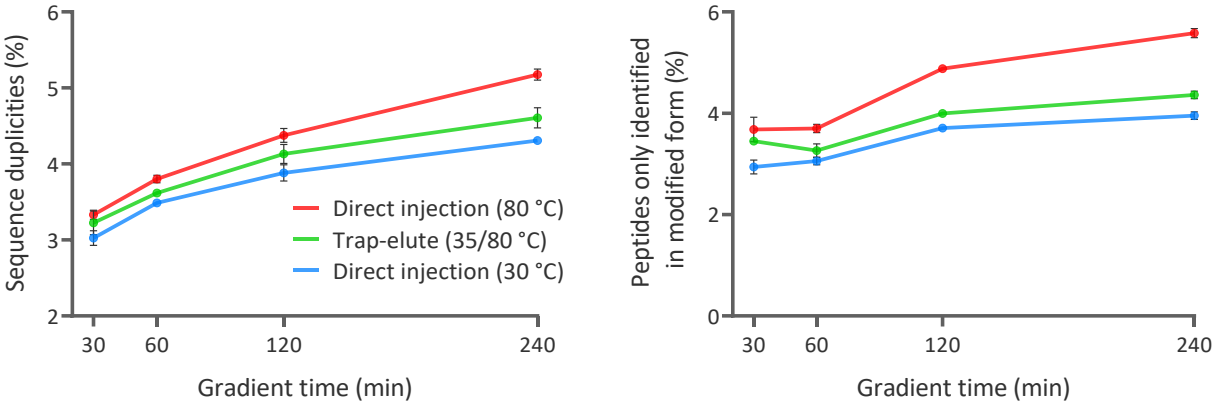

Figure 15: Portion of sequence duplicities and the number of peptides present only in the modified form among all identified peptides in analyses of the Jurkat cell line digest performed using the 1.0 mm i.d. trap-elute setup (35/80 °C) and direct injection on the 1.0 mm i.d. separation column maintained at 30 and 80 °C. Standard deviations smaller than the size of data symbols are not shown.

As shown in the figure, the trap-elute setup reduced the number of sequence duplicities that normally compete for sequencing with intact peptides in the data-dependent acquisition and may "occupy the spot" of another intact peptide with a unique sequence providing extra biological information. This may also explain the increase in the number of identified unique peptide sequences in 120- and 240-min analyses with the installed trap column. Additionally, the trap column installation reduced the number of peptides present only in modified form, which otherwise would not have been identified in case the conventional data search strategy unaware of thermal modifications is applied. Both results prove that the hybrid approach for method comparison was indeed necessary to avoid bias coming from either unadjusted conventional or extended search strategy.

The experiment was carried out using a large mass of injected peptides from a highly complex sample to keep the number of identified peptides as high as possible to gain statistical confidence in the results. DDA experiments rely on a limited number of fragmented peptides per MS1 scan. Therefore, after a certain gain in the injected mass, the number of identifications stops increasing because the number of precursors exceeding the minimum intensity threshold for MS/MS fragmentation has already reached TopN. The injected peptide mass of 2 µg was considered the most reasonable in our experiment. However, when there is a large excess of available precursors at every moment of analysis, the total number of identifications will not suffer from a loss of a few precursors that dropped under the intensity threshold due to peak broadening. That is why we might not have observed the drop in identifications after the trap column installation since its effect on the peak width is very slight, and it has not affected the number of identified peptides because there was still an excess of available precursors. TopN was still reached even if there were slightly fewer precursors due to peak broadening. Therefore, we conducted an experiment involving smaller injection masses to

simulate the conditions when the loss of available precursors would indeed manifest as fewer identifications. By the decrease in the injected peptide mass, the sample complexity was indirectly reduced to avoid oversaturation of MS1 scans and permanent fragmentation of the maximum of allowed precursors. Also, it is a straightforward way to compare method sensitivities by a simple reduction in the analyte concentration. The experiment was also repeated in a reverse order of tested configurations to avoid bias coming from unequal sample age or the time from the latest MS calibration. The single 30-min gradient method was chosen to avoid the influence of temperature- and analysis time-related modification on the number of identifications. The number of unique peptide sequences was again used to compare the method sensitivity (Figure 16):

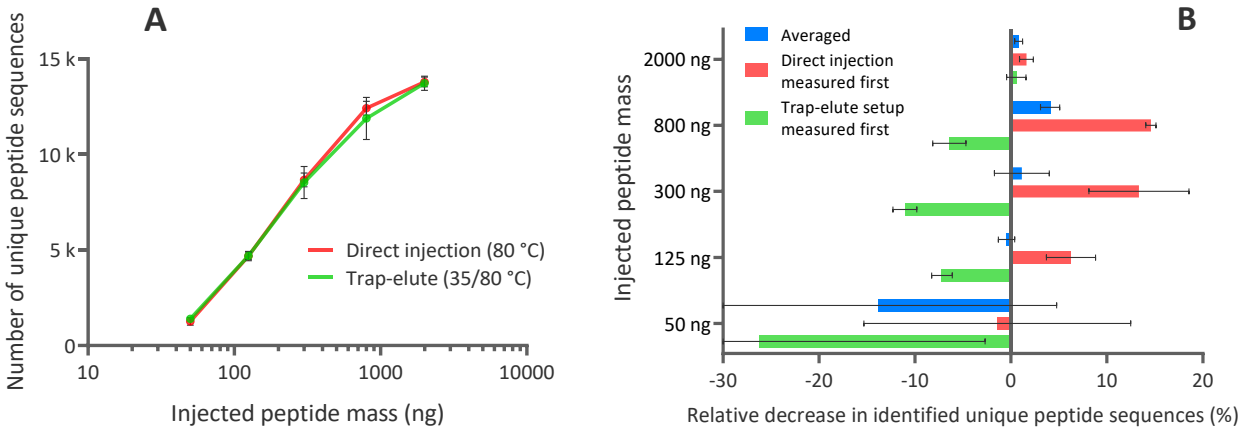

Figure 16: (A) The number of unique peptide sequences identified in 30-min separations of different injected peptide masses using the 1.0 mm i.d. trap-elute setup (35/80 °C) and direct injection on the separation column maintained at 80 °C. The data from experiments with both orders of the tested configurations are averaged. The X-axis has a log 10 scale. **(B)** The relative drop in identifications after the trap column installation normalized to the direct injection (80 °C). The positive percentual change stands for fewer identified unique peptide sequences with the trap-elute setup. The relative changes from experiments with both orders of the tested configurations are shown first and then averaged to obtain a conclusive measure.

Based on the number of identifications, we conclude that the slight peak broadening observed during the trap-elute setup development eventually had a negligible effect on the method sensitivity, and the trap-elute setup preserved the productivity of the direct injection configuration. Only for the injected mass of 800 ng, we observed a noticeable drop in identifications (4.1% on average). For the other injected masses, it does not exceed 1.2%. The increase in identifications in the separation of 50 ng with the trap column should be considered experimental deviation because the trap column can not contribute in this way up to that extent, especially in a short 30-min analysis.

5.4. Application 2: Multi-Attribute LC-MS Method for Characterization of Therapeutic Proteins

The second test application represents a quantitation-oriented analysis of a sample of low complexity. Up to this experiment, the characterization of the trap-elute setup was performed using a simple measure of the number of identified peptides. This approach is reliable, provided that peptide sets are large enough to ensure statistical confidence. However, it is a one-sided evaluation and does not serve as a comprehensive assessment. To make it orthogonal and to expand the method application scope, the experiment involved therapeutic proteins. We were also motivated to observe the quantities of single peptides since it remained unclear if the trap column installation can reduce the formation of certain modifications, for instance, Met oxidation, in short analyses. The sample preparation protocol and LC-MS analysis were designed to mimic a common MAM for the characterization of therapeutic proteins. It exploits the 2.1 mm i.d. trap-elute setup, again compared to direct injection on the separation column maintained at the low and the high temperature. The data evaluation strategy was aimed at the modifications that are degradation sites commonly characterized by manufacturers due to their impact on product quality. We selected only those modifications that were previously shown to be formed during LC-MS analyses, not only during drug production or storage. We also selected a sample preparation protocol with minimum artifact formation to reduce the quantity of sample preparation-related artifacts in our experiment. For each protein, several modification sites were selected either based on previous general studies reporting the influence of these modifications on drug efficiency or safety (*for a review, see* [30]) or using studies involving quantitation of modifications formed on specific degradation sites as the CQAs in the analyzed therapeutic proteins [105]–[109].

We compared peak areas of the artifacts identified in the three datasets and normalized them to the artifact quantity observed in the analyses using direct injection on the separation column maintained at 80 °C (Figure 17):

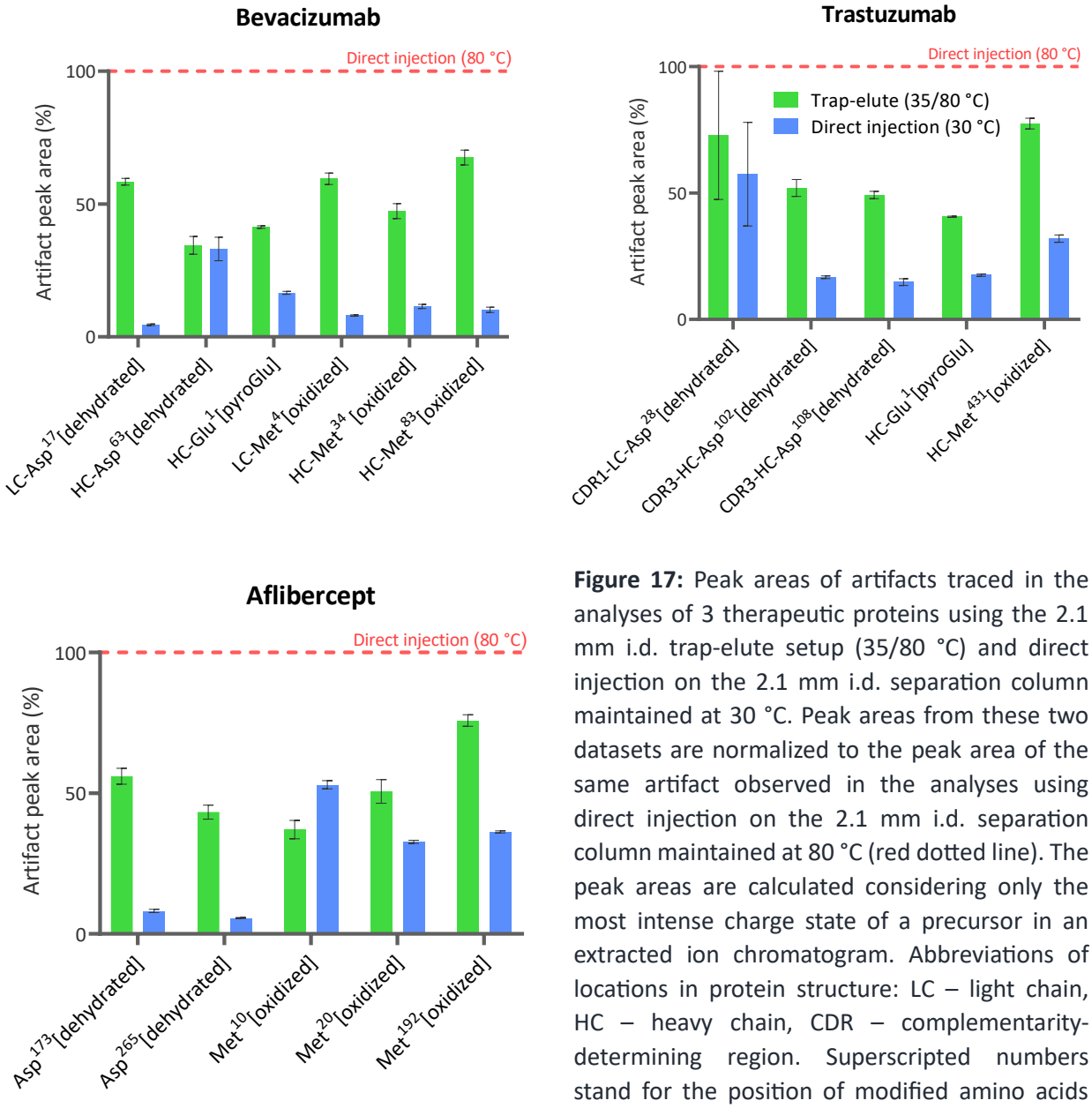

Figure 17: Peak areas of artifacts traced in the analyses of 3 therapeutic proteins using the 2.1 mm i.d. trap-elute setup (35/80 °C) and direct injection on the 2.1 mm i.d. separation column maintained at 30 °C. Peak areas from these two datasets are normalized to the peak area of the same artifact observed in the analyses using direct injection on the 2.1 mm i.d. separation column maintained at 80 °C (red dotted line). The peak areas are calculated considering only the most intense charge state of a precursor in an extracted ion chromatogram. Abbreviations of locations in protein structure: LC – light chain, HC – heavy chain, CDR – complementarity-determining region. Superscripted numbers stand for the position of modified amino acids from the N-terminus.

For most degradation sites, the reduction in artifact quantity after the trap column installation was shown to be at least half of the hypothetical maximum decrease to the modification level observed in the analyses at 30 °C. Thus, the improvement in the number of identified peptides indeed correlates with decreased quantities of single artifacts after visual expertise of chromatograms. The experiment also made clear the improvement in the Met oxidation rate that was not that evident for short analyses in the first test application.

For illustration, we also calculated the percentage of the artifact peak area from the intact peptide peak area for one of the most attention-grabbing artifacts in antibody structure as well as the average peak width of the given intact peptide under the three experimental

conditions (*Figure S4 in Supp. Materials*). It demonstrates how the proposed trap-elute setup can preserve the improved peak shape of peptides as an effect of applied elevated column temperature but minimize the quantity of generated artifacts. In another example, the trap column installation prevented the modification of a substantial portion of a tryptic peptide with N-terminal Gln, resulting in the peak height of the intact peptide unmatched by the direct injection configuration (*Figure S5 in Supp. Materials*). On the other hand, there was no improvement in ammonia loss from Asn as significant as for other modifications, which is in line with the previous findings from the first test application. Collectively, this modification was shown to be less dependent on the column temperature, which also explains only a small difference associated with the trap column installation both in the number of identified artifacts and their quantities.

Based on the results, we assume that a certain quantity of artifacts observed in several previous studies exploiting high-temperature LC methods comes particularly from the in-column modification, besides the actual artifacts of interest generated before the LC analysis [46][109]–[112]. We suggest that the reliability of results in such works might be improved via the implementation of the proposed trap-elute setup with differential column heating. At the same time, the trap-elute setup may enable the utilization of elevated column temperature in analyses of therapeutic proteins, where it has been restricted because of extensive artifact formation. For practitioners who avoid elevated column temperatures for other reasons in the quality control of biopharmaceuticals, it makes adopting this feature more beneficial (e.g., for improvement in the new peak detection). Hypothetically, for the modifications that were particularly efficiently reduced by the trap-elute setup (e.g., Asp dehydration or pyroGlu formation), it may serve as an indicator of the artifact origin: the analysis with and without the trap column would demonstrate if the artifact fully originates from the pre-LC-MS phase (observed artifact quantity is constant regardless of the presence of the trap column) or some portion of it is formed during the analysis (artifact quantity drops with the installation of the trap column).

Additionally, we speculate that if the temperature of the separation column was lowered, for instance, to 60°C, the entire modification extent using the trap-elute setup would drop to that observed in analyses with the direct injection at 30°C. Using the separation column temperature of 80°C, the trap column fails to reduce artifact formation to the lowest possible level, which is desirable in the case of biopharmaceuticals. This lowering of the separation column temperature would also increase the difference between the trap and separation column retentivity, neglecting the residual peak broadening after the trap column installation observed in our experiments. It would also enable to use the trap column at ambient temperature without the necessity to acquire an additional thermostat. Thus, a user may tune the temperature regime based on the analysis aims: either to keep the separation column at 70-80 °C and obtain the superior separation performance but sacrifice peptide intactness to a moderate extent or to keep the modification extent at the “baseline” and profit from lower, but still elevated column temperature of 50-60 °C. The study provides a simple method for the selection of the optimal temperature regime using a standard peptide set. More importantly, it demonstrates several signs of the correct temperature choice, as well as the relationships that define the trap-elute system efficiency.

6. CONCLUSION

Current LC-MS-based bottom-up proteomics needs more efficient chromatographic separation to keep up with the advances in mass spectrometry and to fully exploit the capabilities of state-of-the-art MS instruments. Elevated column temperature represents an attractive means for the improvement of separation performance. However, it also promotes the artificial modification of peptides that, in numerous ways, compromises the outputs of proteomic analyses. The study aimed to develop a high-temperature LC-MS method for bottom-up proteomic analyses that would preserve the benefits of elevated column temperature but minimize artifact formation. The method relies on the installation of a less retentive upstream trap column maintained at a lower temperature. Inspired by traditional trap-elute setups in nanoLC but motivated to exploit the benefits of the higher-flow regime, we developed trap-elute setups for 1.0 and 2.1 mm i.d. column formats. The trap-elute setup was optimized so that peptides spent the maximum part of the analysis being retained in the trap column but still eluted with a peak shape comparable to the direct injection.

The concept efficiency was examined via exploratory LC-MS analyses of whole-cell digests. Although the trap column installation failed to reduce artifact formation to the achievable minimum observed in analysis at low column temperature, we observed more than a 50% drop in the extent of most modification reactions, especially in long-gradient analyses. The clear improvement in Met oxidation rate was observed only in quantities of single artifacts identified in analyses of therapeutic proteins. The modification extent followed a similar trend in the mimicked MAM for the characterization of biopharmaceuticals. This enables safer utilization of elevated column temperature in this field and extends a potential applicability spectrum of the trap-elute setup. Using the trap-elute setup, we identified the same number of unique peptide sequences, which indicates preserved separation performance, and observed modification extent typical for significantly lower column temperatures. Method sensitivity was shown to be almost preserved at different peptide concentration levels. We also observed a significant drop in the number of sequence duplicities and the peptides present only in a modified form, both considered common issues arising from the use of elevated column temperature.

We present an easy-to-introduce concept that increases the profitability of elevated column temperature. We speculate that if the separation column temperature was slightly lowered, the trap column could be efficiently used at ambient temperature, which makes the concept affordable even with a single-column thermostat available. This is also likely the way to approach the minimum of formed artifacts while using a lower but still elevated temperature of the separation column. This would enable the use of elevated column temperature in analyses with zero tolerance for analysis-related artifacts. The concept can be easily adapted for nanoLC that traditionally exploits trap-elute setups. Finally, the trap column also functions as a guard column, preventing the clogging of the separation column. In the future, we plan to adapt the method for online solid-phase extraction via the introduction of a T-piece upstream of the capillary connecting the trap and separation column, which will divert the flow from the trap column to waste during the sample wash step [12].

7. REFERENCES

[1] R. Aebersold and M. Mann, “Mass-spectrometric exploration of proteome structure and function,” *Nature*, vol. 537, pp. 347–355, 2016, doi: 10.1038/nature19949.

[2] E. Shishkova, A. S. Hebert, and J. J. Coon, “Now, More Than Ever, Proteomics Needs Better Chromatography,” *Cell Syst*, vol. 3, no. (4), pp. 321–324, 2016, doi: 10.1016/j.cels.2016.10.007.

[3] J. Lenčo, T. Šemlej, M. A. Khalikova, I. Fabrik, and F. Švec, “Sense and Nonsense of Elevated Column Temperature in Proteomic Bottom-up LC-MS Analyses,” *J Proteome Res*, vol. 20, no. 1, pp. 420–432, Jan. 2021, doi: 10.1021/acs.jproteome.0c00479.

[4] U. Dieter Neue, “Peak capacity in unidimensional chromatography,” *J Chromatogr A*, vol. 1184, pp. 107–130, 2008, doi: 10.1016/j.chroma.2007.12.005.

[5] T. Teutenberg, “Potential of high temperature liquid chromatography for the improvement of separation efficiency - A review,” *Anal Chim Acta*, vol. 643, pp. 1–12, 2009, doi: 10.1016/j.aca.2009.04.008.

[6] S. Heinisch and J.-L. Rocca, “Sense and nonsense of high-temperature liquid chromatography,” *J Chromatogr A*, vol. 1216, pp. 642–658, 2009, doi: 10.1016/j.chroma.2008.11.048.

[7] E. R. Stadtman, H. Van Remmen, A. Richardson, N. B. Wehr, and R. L. Levine, “Methionine oxidation and aging,” *Biochim Biophys Acta*, vol. 1703, pp. 135–140, 2005, doi: 10.1016/j.bbapap.2004.08.010.

[8] M. L. Moro *et al.*, “Pyroglutamate and Isoaspartate modified Amyloid-Beta in ageing and Alzheimer’s disease,” *Acta Neuropathol Commun*, vol. 6, no. 3, Jan. 2018, doi: 10.1186/s40478-017-0505-x.

[9] D. Wang, C. Nowak, B. Mason, A. Katiyar, and H. Liu, “Analytical artifacts in characterization of recombinant monoclonal antibody therapeutics,” *J Pharm Biomed Anal*, vol. 183, May 2020, doi: 10.1016/J.JPBA.2020.113131.

[10] M. Chul Jung and M. Wanninger, “Considerations for Selecting the Optimal Stationary Phases for Proteomic Trap-and-Elute Nanochromatography,” *White Paper, Waters, 2017, 720006063EN.*

[11] J. Lenčo *et al.*, “Reversed-Phase Liquid Chromatography of Peptides for Bottom-Up Proteomics: A Tutorial,” *J Proteome Res*, vol. 21, no. 12, pp. 2846–2892, Dec. 2022, doi: 10.1021/acs.jproteome.2c00407.

[12] L. J. Licklider, C. C. Thoreen, J. Peng, and S. P. Gygi, “Automation of Nanoscale Microcapillary Liquid Chromatography-Tandem Mass Spectrometry with a Vented Column,” *Anal Chem*, vol. 71, no. 13, pp. 3076–3083, 2002, doi: 10.1021/ac025529o.

[13] M. A. Lauber, S. M. Koza, and K. J. Fountain, “Optimizing Peak Capacity in Nanoscale Trap-Elute Peptide Separations with Differential Column Heating,” Application Note, Waters, May 2014, 720005047.

[14] J. Lenčo *et al.*, “Conventional-Flow Liquid Chromatography-Mass Spectrometry for Exploratory Bottom-Up Proteomic Analyses,” *Anal Chem*, vol. 90, no. 8, pp. 5381–5389, Apr. 2018, doi: 10.1021/acs.analchem.8b00525.

[15] Y. Bian *et al.*, “Robust, reproducible and quantitative analysis of thousands of proteomes by micro-flow LC-MS/MS,” *Nat Commun*, vol. 11, no. 1, p. 157, 2020, doi: 10.1038/s41467-019-13973-x.

[16] F. Yang *et al.*, “Mass spectrometry-based multi-attribute method in protein therapeutics product quality monitoring and quality control,” *MAbs*, vol. 15, no. 1, 2023, doi: 10.1080/19420862.2023.2197668.

[17] D. S. ; Bell, “Perspectives on the Adoption and Utility of 1.0-mm Internal Diameter Liquid Chromatography Columns,” *LCGC Europe*, vol. 32, no. 3, pp. 140–143, 2019, Accessed: Nov. 11, 2023. [Online]. Available: https://www.chromatographyonline.com/view/perspectives-adoption-and-utility-10-mm-internal-diameter-liquid-chromatography-columns

[18] Y. Bian, C. Gao, and B. Kuster, “On the potential of micro-flow LC-MS/MS in proteomics,” *Expert Rev Proteomics*, vol. 19, no. 3, pp. 153–164, 2022, doi: 10.1080/14789450.2022.2134780.

[19] J. Dittrich, S. Becker, M. Hecht, and U. Ceglarek, “Sample preparation strategies for targeted proteomics via proteotypic peptides in human blood using liquid chromatography tandem mass spectrometry,” *Proteomics Clin Appl*, vol. 9, no. 1–2, pp. 5–16, Feb. 2015, doi: 10.1002/prca.201400121.

[20] J. D. Lambris, “Sample Preparation Strategies for Proteomics,” in *Modern Proteomics - Sample Preparation, Analysis and Practical Applications*, vol. 919, 2016, pp. 3–143. doi: 10.1007/978-3-319-41448-5.

[21] J. M. Burkhart, C. Schumbrutzki, S. Wortelkamp, A. Sickmann, and R. P. Zahedi, “Systematic and quantitative comparison of digest efficiency and specificity reveals the impact of trypsin quality on MS-based proteomics,” *J Proteomics*, vol. 75, no. 4, pp. 1454–1462, Feb. 2012, doi: 10.1016/J.JPROT.2011.11.016.

[22] P. Jandera and J. Churáček, “Gradient elution in liquid chromatography : I. The influence of the composition of the mobile phase on the capacity ratio (retention volume, band width, and resolution) in isocratic elution — theoretical considerations,” *J Chromatogr A*, vol. 91, pp. 207–221, Apr. 1974, doi: 10.1016/S0021-9673(01)97901-4.

[23] L. R. Snyder, J. W. Dolan, and J. R. Gant, “Gradient elution in high-performance liquid chromatography : I. Theoretical basis for reversed-phase systems,” *J Chromatogr A*, vol. 165, no. 1, pp. 3–30, Mar. 1979, doi: 10.1016/S0021-9673(00)85726-X.

[24] C. T. Mant, T. W. L. Burke, and R. S. Hodges, “Optimization of Peptide Separations in Reversed-Phase HPLC: Isocratic Versus Gradient Eiution,” *Chromatographia*, vol. 24, pp. 565–572, 1987.

[25] J. Koyama, J. Nomura, Y. Shiojima, Y. Ohtsu, and I. Horii, “Effect of column length and elution mechanism on the separation of proteins by reversed-phase high-performance liquid chromatography,” *J Chromatogr A*, vol. 625, no. 2, pp. 217–222, Nov. 1992, doi: 10.1016/0021-9673(92)85205-8.

[26] M. Gilar, P. Olivova, A. E. Daly, and J. C. Gebler, “Two-dimensional separation of peptides using RP-RP-HPLC system with different pH in first and second separation dimensions,” *J Sep Sci*, vol. 28, no. 14, pp. 1694–1703, Sep. 2005, doi: 10.1002/JSSC.200500116.

[27] M. Gilar, P. Olivova, A. E. Daly, and J. C. Gebler, “Orthogonality of Separation in Two-Dimensional Liquid Chromatography,” *Anal Chem*, vol. 77, no. 19, pp. 6426–6434, Oct. 2005, doi: 10.1021/AC050923I.

[28] D. Yeung *et al.*, “Separation Orthogonality in Liquid Chromatography-Mass Spectrometry for Proteomic Applications: Comparison of 16 Different Two-Dimensional Combinations,” *Anal Chem*, vol. 92, no. 5, pp. 3904–3912, Mar. 2020, doi: 10.1021/acs.analchem.9b05407.

[29] S. Ramazi and J. Zahiri, “Post-translational modifications in proteins: resources, tools and prediction methods,” *Database*, vol. 2021, 2021, doi: 10.1093/database/baab012.

[30] L. K. Hmiel, K. A. Brorson, and M. T. Boyne, “Post-translational structural modifications of immunoglobulin G and their effect on biological activity,” *Anal Bioanal Chem*, vol. 407, no. 1, pp. 79–94, Jan. 2015, doi: 10.1007/s00216-014-8108-x.

[31] N. Alt *et al.*, “Determination of critical quality attributes for monoclonal antibodies using quality by design principles,” *Biologicals*, vol. 44, pp. 291–305, 2016, doi: 10.1016/j.biologicals.2016.06.005.

[32] M. Den Ridder, E. Knibbe, W. Van Den Brandeler, P. Daran-Lapujade, and M. Pabst, “A systematic evaluation of yeast sample preparation protocols for spectral identifications, proteome coverage and post-isolation modifications,” *J Proteomics*, vol. 261, pp. 1874–3919, 2022, doi: 10.1016/j.jprot.2022.104576.

[33] J. Lenč, M. A. Khalikova, F. Ek, and S.̌ Vec, “Dissolving Peptides in 0.1% Formic Acid Brings Risk of Artificial Formylation,” *Cite This: J. Proteome Res*, vol. 19, pp. 993–999, 2020, doi: 10.1021/acs.jproteome.9b00823.

[34] P. Hao, Y. Ren, A. J. Alpert, and S. Kwan Sze, “Detection, Evaluation and Minimization of Nonenzymatic Deamidation in Proteomic Sample Preparation,” *Molecular and Cellular Proteomics*, vol. 10, no. 10, 2011, doi: 10.1074/mcp.O111.009381.

[35] L. Zang *et al.*, “Residual metals cause variability in methionine oxidation measurements in protein pharmaceuticals using LC-UV/MS peptide mapping,” *Journal of Chromatography B*, vol. 895–896, pp. 71–76, May 2012, doi: 10.1016/J.JCHROMB.2012.03.016.

[36] D. Chelius *et al.*, “Formation of pyroglutamic acid from N-terminal glutamic acid in immunoglobulin gamma antibodies,” *Anal Chem*, vol. 78, no. 7, pp. 2370–2376, Apr. 2006, doi: 10.1021/AC051827K.

[37] G. C. Chu, D. Chelius, G. Xiao, H. K. Khor, S. Coulibaly, and P. V. Bondarenko, “Accumulation of succinimide in a recombinant monoclonal antibody in mildly acidic buffers under elevated temperatures,” *Pharm Res*, vol. 24, no. 6, pp. 1145–1156, Jun. 2007, doi: 10.1007/S11095-007-9241-4.

[38] L. W. Dick, C. Kim, D. Qiu, and K. C. Cheng, “Determination of the origin of the N-terminal pyro-glutamate variation in monoclonal antibodies using model peptides,” *Biotechnol Bioeng*, vol. 97, no. 3, pp. 544–553, Jun. 2007, doi: 10.1002/BIT.21260.

[39] S. Capasso, A. J. Kirby, S. Salvadori, F. Sicaa, and A. Zagari, “Kinetics and Mechanism of the Reversible lsomerization of Aspartic Acid Residues in Tetrapeptides,” *Chem Soc Perkin Trans*, vol. 2, pp. 437–442, 1995.

[40] M. Xie, D. Vander Velde, M. Morton, R. T. Borchardt, and R. L. Schowen, “pH-induced change in the rate-determining step for the hydrolysis of the Asp/Asn-derived cyclic-imide intermediate in protein degradation,” *J Am Chem Soc*, vol. 118, no. 37, pp. 8955–8956, Sep. 1996, doi: 10.1021/ja9606182.

[41] C. Ming Tsung and H. Fraenkel-Conrat, “Preferential Release of Aspartic Acid by Dilute Acid Treatment of Tryptic Peptides,” *Biochemistry*, vol. 4, no. 5, pp. 793–801, 1963, doi: 10.1021/bi00881a001.

[42] D. Ren *et al.*, “An improved trypsin digestion method minimizes digestion-induced modifications on proteins,” *Anal Biochem*, vol. 392, no. 1, pp. 12–21, Sep. 2009, doi: 10.1016/J.AB.2009.05.018.

[43] J. Richardson and Z. Zhang, “Fully Unattended Online Protein Digestion and LC-MS Peptide Mapping,” *Anal Chem*, vol. 95, pp. 15514–15521, 2023, doi: 10.1021/acs.analchem.3c01554.

[44] P. Jiang, F. Li, and J. Ding, “Development of an efficient LC-MS peptide mapping method using accelerated sample preparation for monoclonal antibodies,” *Journal of Chromatography B*, vol. 1137, p. 121895, Jan. 2020, doi: 10.1016/J.JCHROMB.2019.121895.

[45] M. Cao *et al.*, “An Automated and Qualified Platform Method for Site-Specific Succinimide and Deamidation Quantitation Using Low-pH Peptide Mapping,” *J Pharm Sci*, vol. 108, no. 11, pp. 3540–3549, Nov. 2019, doi: 10.1016/J.XPHS.2019.07.019.

[46] Y. D. Liu *et al.*, “Expanding the Analytical Toolbox: Developing New Lys-C Peptide Mapping Methods with Minimized Assay-Induced Artifacts to Fully Characterize Antibodies,” *Pharmaceuticals 2023, Vol. 16, Page 1327*, vol. 16, no. 9, p. 1327, Sep. 2023, doi: 10.3390/PH16091327.

[47] T. Mouchahoir and J. E. Schiel, “Development of an LC-MS/MS peptide mapping protocol for the NISTmAb,” *Anal Bioanal Chem*, vol. 410, no. 8, pp. 2111–2126, Mar. 2018, doi: 10.1007/s00216-018-0848-6.

[48] M. Beck *et al.*, “The quantitative proteome of a human cell line,” *Mol Syst Biol*, vol. 7, 2011, doi: 10.1038/MSB.2011.82.

[49] F. Meier, P. E. Geyer, S. Virreira Winter, J. Cox, and M. Mann, “BoxCar acquisition method enables single-shot proteomics at a depth of 10,000 proteins in 100 minutes,” *Nat Methods*, vol. 15, pp. 440–448, 2018, doi: 10.1038/s41592-018-0003-5.

[50] N. Nagaraj *et al.*, “Deep proteome and transcriptome mapping of a human cancer cell line,” *Mol Syst Biol*, vol. 7, 2011, doi: 10.1038/MSB.2011.81.

[51] J. Muntel *et al.*, “Surpassing 10 000 identified and quantified proteins in a single run by optimizing current LC-MS instrumentation and data analysis strategy,” *Mol Omics*, vol. 15, p. 348, 2019, doi: 10.1039/c9mo00082h.

[52] K. Sandra, I. Vandenheede, and P. Sandra, “Modern chromatographic and mass spectrometric techniques for protein biopharmaceutical characterization,” *J Chromatogr A*, vol. 1335, pp. 81–103, 2014, doi: 10.1016/j.chroma.2013.11.057.

[53] F. Lermyte, Y. O. Tsybin, P. B. O’Connor, and J. A. Loo, “Top or Middle? Up or Down? Toward a Standard Lexicon for Protein Top-Down and Allied Mass Spectrometry Approaches,” *J Am Soc Mass Spectrom*, vol. 30, no. 7, pp. 1149–1157, Jul. 2019, doi: 10.1007/s13361-019-02201-x.

[54] E. I. Chen, D. Cociorva, J. L. Norris, and J. R. Yates, “Optimization of mass spectrometry-compatible surfactants for shotgun proteomics,” *J Proteome Res*, vol. 6, no. 7, pp. 2529–2538, Jul. 2007, doi: 10.1021/pr060682a.

[55] P. G. Hains and P. J. Robinson, “The Impact of Commonly Used Alkylating Agents on Artifactual Peptide Modification,” *J Proteome Res*, vol. 16, no. 9, pp. 3443–3447, Sep. 2017, doi: 10.1021/acs.jproteome.7b00022.

[56] K. G. Kuznetsova *et al.*, “Cysteine alkylation methods in shotgun proteomics and their possible effects on methionine residues,” *J Proteomics*, vol. 231, p. 104022, Jan. 2021, doi: 10.1016/J.JPROT.2020.104022.

[57] L. Switzar, M. Giera, and W. M. A. Niessen, “Protein digestion: An overview of the available techniques and recent developments,” *Journal of Proteome Research*, vol. 12, no. 3. American Chemical Society, pp. 1067–1077, Mar. 01, 2013. doi: 10.1021/pr301201x.

[58] P. Giansanti, L. Tsiatsiani, T. Y. Low, and A. J. R. Heck, “Six alternative proteases for mass spectrometry–based proteomics beyond trypsin,” *Nat Protoc*, vol. 11, no. 5, pp. 993–1006, Apr. 2016, doi: 10.1038/nprot.2016.057.

[59] J. V. Olsen, S. E. Ong, and M. Mann, “Trypsin cleaves exclusively C-terminal to arginine and lysine residues,” *Molecular and Cellular Proteomics*, vol. 3, no. 6, pp. 608–614, Jun. 2004, doi: 10.1074/mcp.T400003-MCP200.

[60] M. Benore-Parsons, N. G. Seidah, and L. P. Wennogle, “Substrate phosphorylation can inhibit proteolysis by trypsin-like enzymes,” *Arch Biochem Biophys*, vol. 272, no. 2, pp. 274–280, Aug. 1989, doi: 10.1016/0003-9861(89)90220-8.

[61] J. R. Wiśniewski, K. Zettl, M. Pilch, B. Rysiewicz, and I. Sadok, “‘Shotgun’ proteomic analyses without alkylation of cysteine,” *Anal Chim Acta*, vol. 1100, pp. 131–137, Mar. 2020, doi: 10.1016/j.aca.2019.12.007.

[62] “Low Artifact Digestion Buffer,” Technical Bulletin, Sigma-Aldrich, 2018.

[63] “RapiGest SF Accelerated Tryptic Digestion of Proteins,” Application Note, Waters, 2003, WA20774.

[64] S. Millán-Martín *et al.*, “Comparison of Alternative Approaches to Trypsin Protein Digestion for Reproducible and Efficient Peptide Mapping Analysis of Monoclonal Antibodies,” Application Note 21782, Thermo Fisher Scientific, 2018, AN21782-EN 0718S.

[65] K. Meyer and M. Oliver, “Simple and sensitive quantitation of large therapeutic proteins in plasma in 90 minutes,” Application Note 22059, Thermo Fisher Scientific, 2020, AN22059-EN 0620S.

[66] K. Stejskal, D. Potěšil, and Z. Zdráhal, “Suppression of peptide sample losses in autosampler vials,” *J Proteome Res*, vol. 12, no. 6, pp. 3057–3062, Jun. 2013, doi: 10.1021/pr400183v.

[67] A. N. Hoofnagle *et al.*, “Recommendations for the Generation, Quantification, Storage, and Handling of Peptides Used for Mass Spectrometry-Based Assays,” *Clin Chem*, vol. 62, no. 1, pp. 48–69, 2016, doi: 10.1373/clinchem.2015.250563.

[68] P. C. Iraneta, K. D. Wyndham, D. R. Mccabe, and T. H. Walter, “A Review of Waters Hybrid Particle Technology. Part 3. Charged Surface Hybrid (CSH) Technology and Its Use in Liquid Chromatography,” White Paper, Waters, 2021, 720003929EN.

[69] Z. Kadlecová, P. Kozlík, E. Tesařová, M. Gilar, and K. Kalíková, “Characterization and comparison of mixed-mode and reversed-phase columns; interaction abilities and applicability for peptide separation,” *J Chromatogr A*, vol. 1648, p. 462182, Jul. 2021, doi: 10.1016/J.CHROMA.2021.462182.

[70] M. A. Lauber, S. M. Koza, S. A. Mccall, B. A. Alden, P. C. Iraneta, and K. J. Fountain, “High-Resolution Peptide Mapping Separations with MS-Friendly Mobile Phases and Charge-Surface-Modified C18,” *Anal. Chem*, vol. 85, p. 22, 2013, doi: 10.1021/ac401481z.

[71] F. Gritti, K. Horvath, and G. Guiochon, “How changing the particle structure can speed up protein mass transfer kinetics in liquid chromatography,” *J Chromatogr A*, vol. 1263, pp. 84–98, 2012, doi: 10.1016/j.chroma.2012.09.030.

[72] A. Michalski, J. Cox, and M. Mann, “More than 100,000 detectable peptide species elute in single shotgun proteomics runs but the majority is inaccessible to data-dependent LC-MS/MS,” *J Proteome Res*, vol. 10, no. 4, pp. 1785–1793, Apr. 2011, doi: 10.1021/pr101060v.

[73] P. L. Urban, “Clarifying Misconceptions about Mass and Concentration Sensitivity,” *J Chem Educ*, vol. 93, no. 6, pp. 984–987, Jun. 2016, doi: 10.1021/ACS.JCHEMED.5B00986.

[74] J. Šesták, D. Moravcová, and V. Kahle, “Instrument platforms for nano liquid chromatography,” *J Chromatogr A*, vol. 1421, pp. 2–17, Nov. 2015, doi: 10.1016/J.CHROMA.2015.07.090.

[75] E. J. Hsieh, M. S. Bereman, S. Durand, G. A. Valaskovic, and M. J. MacCoss, “Effects of column and gradient lengths on peak capacity and peptide identification in nanoflow LC-MS/MS of complex proteomic samples,” *J Am Soc Mass Spectrom*, vol. 24, no. 1, pp. 148–153, Jan. 2013, doi: 10.1007/S13361-012-0508-6.

[76] A. E. Reising, J. M. Godinho, J. Bernzen, J. W. Jorgenson, and U. Tallarek, “Axial heterogeneities in capillary ultrahigh pressure liquid chromatography columns: Chromatographic and bed morphological characterization,” *J Chromatogr A*, vol. 1569, pp. 44–52, Sep. 2018, doi: 10.1016/J.CHROMA.2018.07.037.

[77] S. Eeltink, S. Dolman, F. Detobel, R. Swart, M. Ursem, and P. J. Schoenmakers, “High-efficiency liquid chromatography–mass spectrometry separations with 50 mm, 250 mm, and 1 m long polymer-based monolithic capillary columns for the characterization of complex proteolytic digests,” *J Chromatogr A*, vol. 1217, no. 43, pp. 6610–6615, Oct. 2010, doi: 10.1016/J.CHROMA.2010.03.037.

[78] N. B. Cech and C. G. Enke, “Practical implications of some recent studies in electrospray ionization fundamentals,” *Mass Spectrom Rev*, vol. 20, no. 6, pp. 362–387, Jan. 2001, doi: 10.1002/MAS.10008.

[79] S. Å. Gustavsson, J. Samskog, K. E. Markides, and B. Långström, “Studies of signal suppression in liquid chromatography–electrospray ionization mass spectrometry using volatile ion-pairing reagents,” *J Chromatogr A*, vol. 937, no. 1–2, pp. 41–47, Dec. 2001, doi: 10.1016/S0021-9673(01)01328-0.

[80] S. Jadeja, R. Kupcik, I. Fabrik, H. Sklenářová, and J. Lenčo, “A stationary phase with a positively charged surface allows for minimizing formic acid concentration in the mobile phase, enhancing electrospray ionization in LC-MS proteomic experiments,” *Analyst*, vol. 148, pp. 5980–5990, 2023, doi: 10.1039/d3an01508d.

[81] R. Nogueira, M. Lämmerhofer, and W. Lindner, “Alternative high-performance liquid chromatographic peptide separation and purification concept using a new mixed-mode reversed-phase/weak anion-exchange type stationary phase,” *J Chromatogr A*, vol. 1089, pp. 158–169, 2005, doi: 10.1016/j.chroma.2005.06.093.

[82] R. E. Birdsall, J. Kellett, Y. Q. Yu, and W. Chen, “Application of mobile phase additives to reduce metal-ion mediated adsorption of non-phosphorylated peptides in RPLC/MS-based assays,” *Journal of Chromatography B*, vol. 1126–1127, p. 121773, 2019, doi: 10.1016/j.jchromb.2019.121773.

[83] Bigos P, Birdsall R E, and Walter T H, “MaxPeak Premier Solutions: Improving Consumer Safety Through Innovative Science,” White Paper, Waters, 2023, 720008054EN.

[84] E. Defossez, J. Bourquin, S. von Reuss, S. Rasmann, and G. Glauser, “Eight key rules for successful data-dependent acquisition in mass spectrometry-based metabolomics,” *Mass Spectrom Rev*, vol. 42, no. 1, pp. 131–143, Jan. 2023, doi: 10.1002/mas.21715.

[85] R. B. Kitata, J. C. Yang, and Y. J. Chen, “Advances in data-independent acquisition mass spectrometry towards comprehensive digital proteome landscape,” *Mass Spectrom Rev*, Nov. 2022, doi: 10.1002/MAS.21781.

[86] F. Zhang, W. Ge, G. Ruan, X. Cai, and T. Guo, “Data-Independent Acquisition Mass Spectrometry-Based Proteomics and Software Tools: A Glimpse in 2020,” *Proteomics*, vol. 20, pp. 17–18, 2020, doi: 10.1002/pmic.201900276.

[87] Á. Révész *et al.*, “Selection of Collision Energies in Proteomics Mass Spectrometry Experiments for Best Peptide Identification: Study of Mascot Score Energy Dependence Reveals Double Optimum,” *J Proteome Res*, vol. 17, pp. 1898–1906, 2018, doi: 10.1021/acs.jproteome.7b00912.

[88] Á. Révész *et al.*, “Tailoring to Search Engines: Bottom-Up Proteomics with Collision Energies Optimized for Identification Confidence,” *J Proteome Res*, vol. 20, no. 1, pp. 474–484, Jan. 2021, doi: 10.1021/acs.jproteome.0c00518.

[89] A. I. Nesvizhskii, O. Vitek, and R. Aebersold, “Analysis and validation of proteomic data generated by tandem mass spectrometry,” *Nature Methods*, vol. 4, no. 10. pp. 787–797, Oct. 2007. doi: 10.1038/nmeth1088.

[90] L. K. Pino, B. C. Searle, J. G. Bollinger, B. Nunn, B. Maclean, and M. J. Maccoss, “The Skyline Ecosystem: Informatics for Quantitative Mass Spectrometry Proteomics,” *Mass Spectrom Rev.*, vol. 39, no. 3, pp. 229–244, 2020, doi: 10.1002/mas.21540.

[91] A. I. Nesvizhskii, “A survey of computational methods and error rate estimation procedures for peptide and protein identification in shotgun proteomics,” *Journal of Proteomics*, vol. 73, no. 11. pp. 2092–2123, Oct. 10, 2010. doi: 10.1016/j.jprot.2010.08.009.

[92] M. Bern, Y. J. Kil, and C. Becker, “Byonic: Advanced peptide and protein identification software,” *Curr Protoc Bioinformatics*, vol. Chapter 13.20.1-14, 2012, doi: 10.1002/0471250953.bi1320s40.

[93] J. E. Elias and S. P. Gygi, “Target-decoy search strategy for increased confidence in large-scale protein identifications by mass spectrometry,” *Nat Methods*, vol. 4, no. 3, pp. 207–214, Feb. 2007, doi: 10.1038/nmeth1019.

[94] M. W. Bern and Y. J. Kil, “Two-dimensional target decoy strategy for shotgun proteomics,” *J Proteome Res*, vol. 10, no. 12, pp. 5296–5301, Dec. 2011, doi: 10.1021/pr200780j.

[95] E. V. Moskovets and A. R. Ivanov, “Comparative studies of peak intensities and chromatographic separation of proteolytic digests, PTMs, and intact proteins obtained by nanoLC-ESI MS analysis at room and elevated temperatures,” *Anal Bioanal Chem*, vol. 408, no. 15, pp. 3953–3968, Jun. 2016, doi: 10.1007/S00216-016-9386-2.

[96] S. E. Farias, K. G. Kline, J. Klepacki, and C. C. Wu, “Quantitative improvements in peptide recovery at elevated chromatographic temperatures from microcapillary liquid chromatography-mass spectrometry analyses of brain using selected reaction monitoring,” *Anal Chem*, vol. 82, no. 9, pp. 3435–3440, May 2010, doi: 10.1021/AC100359P.

[97] J. C. Gesquiere, E. Diesis, M. T. Cung, and A. Tartar, “Slow isomerization of some proline-containing peptides inducing peak splitting during reversed-phase high-performance liquid chromatography,” *J Chromatogr A*, vol. 478, no. C, pp. 121–129, Jan. 1989, doi: 10.1016/0021-9673(89)90010-1.

[98] J. A. Pascual, G. J. Ten Hove, and A. P. J. M. De Jong, “Development of a Precolumn Capillary Liquid Chromatography Switching System for Coupling to Mass Spectrometry,” *Journal of Microcolumn Separations*, vol. 8, no. 6, pp. 383–387, 1996, doi: 10.1002/(SICI)1520-667X(1996)8:6<383::AID-MCS2>3.0.CO;2-Y.

[99] M. Rogeberg, H. Malerod, H. Roberg-Larsen, C. Aass, and S. R. Wilson, “On-line solid phase extraction-liquid chromatography, with emphasis on modern bioanalysis and miniaturized systems,” *J Pharm Biomed Anal*, vol. 87, pp. 120–129, 2014, doi: 10.1016/j.jpba.2013.05.006.

[100] A. Peterson, L. Hohmann, L. Huang, B. Kim, J. K. Eng, and D. B. Martin, “Analysis of RP-HPLC loading conditions for maximizing peptide identifications in shotgun proteomics,” *J Proteome Res*, vol. 8, no. 8, pp. 4161–4168, Aug. 2009, doi: 10.1021/PR9001417.

[101] G. Mitulović, M. Smoluch, J. P. Chervet, I. Steinmacher, A. Kungl, and K. Mechtler, “An improved method for tracking and reducing the void volume in nano HPLC-MS with micro trapping columns,” *Anal Bioanal Chem*, vol. 376, no. 7, pp. 946–951, Aug. 2003, doi: 10.1007/S00216-003-2047-2.

[102] S. Wang *et al.*, “Simple Approach for Improved LC-MS Analysis of Protein Biopharmaceuticals via Modification of Desolvation Gas,” *Anal Chem*, 2019, doi: 10.1021/acs.analchem.8b05846.

[103] “Pierce™ Peptide Desalting Spin Columns,” User Guide, Thermo Fisher Scientific, 2017, MAN0017280.

[104] M. Heidorn, “Optimization of Chromatographic Results by Using Mobile Phase Preheating,” Technical Note 150, Waters, 2016.

[105] Betgovargez E *et al.*, “Comprehensive Characterization of Trastuzumab using a Single-Shot Peptide Mapping Approach with CESI-MS,” Application Note, Sciex, 2014.

[106] B. Gürel *et al.*, “Optimized Methods for Analytical and Functional Comparison of Biosimilar mAb Drugs: A Case Study for Avastin, Mvasi, and Zirabev,” *Sci Pharm*, vol. 90, no. 2, Jun. 2022, doi: 10.3390/scipharm90020036.

[107] Y. F. K. Dyck *et al.*, “Forced Degradation Testing as Complementary Tool for Biosimilarity Assessment,” *Bioengineering*, vol. 6, no. 3, p. 62, Jul. 2019, doi: 10.3390/bioengineering6030062.

[108] S. L. Chen, S. L. Wu, L. J. Huang, J. B. Huang, and S. H. Chen, “A global comparability approach for biosimilar monoclonal antibodies using LC-tandem MS based proteomics,” *J Pharm Biomed Anal*, vol. 80, pp. 126–135, Jun. 2013, doi: 10.1016/j.jpba.2013.02.040.

[109] H. Xie *et al.*, “Rapid comparison of a candidate biosimilar to an innovator monoclonal antibody with advanced liquid chromatography and mass spectrometry technologies,” *MAbs*, vol. 2, no. 4, pp. 379–394, 2010, doi: 10.4161/mabs.11986.

[110] Z. Hao *et al.*, “Multi-attribute method performance profile for quality control of monoclonal antibody therapeutics,” *J Pharm Biomed Anal*, vol. 205, Oct. 2021, doi: 10.1016/j.jpba.2021.114330.

[111] Y. E. Song *et al.*, “Automated mass spectrometry multi-attribute method analyses for process development and characterization of mAbs,” *J Chromatogr B Analyt Technol Biomed Life Sci*, vol. 1166, Mar. 2021, doi: 10.1016/j.jchromb.2021.122540.

[112] X. Li *et al.*, “High throughput peptide mapping method for analysis of site specific monoclonal antibody oxidation,” *J Chromatogr A*, vol. 1460, pp. 51–60, Aug. 2016, doi: 10.1016/j.chroma.2016.06.085.

8. SUPPLEMENTARY MATERIALS

Table S1: Ion source parameters applied in distinct experiments in accordance with used mobile phase flow rate (auto-default):

	Microbore 1.0 mm i.d. columns		Narrow-bore 2.1 mm i.d. columns
Mobile phase flow rate	50 µL/min	68 µL/min	300 µL/min
Ion Source Parameter			
Sheath gas flow rate, arb. units	30.0	32.0	48.0
Aux gas flow rate, arb. units	10.0	10.0	11.0
Sweep gas flow rate, arb. units	1.0	1.0	2.0
Spray voltage, kV	3.5	3.5	3.5
Capillary temperature, °C	250.0	250.0	256.0
Funnel radio frequency level	60.0	50.0	50.0
Aux gas heater temperature, °C	150.0	168.0	413.0
Depth of the ESI probe	A	A	halfway between B-C

Table S2: Parameters of MS1 filtering, DDA, and MS/MS acquisition.

4.2.2. Trap Column Selection and Optimization of Analytical Conditions	
MS1 settings	
Polarity	positive
Resolution at 200 m/z	60 000
AGC target	3×10^6
Maximum injection time	110 ms
Scan range	350 to 1500 m/z
4.2.3. Proof of Hypothesis: LC-MS Analysis of a Whole-Cell Proteome with Integration of Trap-Elute Setup	
MS1 settings	
Polarity	positive
Resolution at 200 m/z	60 000
AGC target	3×10^6
Maximum injection time	110 ms
Scan range	350 to 1500 m/z
DDA and MS2 settings	
TopN	10
Precursor charge states excluded from fragmentation	1, 6-8, >8
Intensity threshold	1×10^5
Isolation window	1.8 m/z
Isolation offset	0.3 m/z

Table S2: Parameters of MS1 filtering, DDA, and MS/MS acquisition. (*Continued*)

Normalized collision energy for HCD	27
Resolution at 200 m/z	15 000
AGC target	2×10^5
Maximum injection time	50 ms
Exclusion isotopes	On
Dynamic exclusion time	20.0 s
Chromatographic peak width	4 s
Apex trigger	-
Fragmentation of charge states	Single charge state, the most intense
4.2.4. Test Application 1: Exploratory Microflow LC-MS Analysis of Jurkat Cell Line Proteome	
MS1 settings	
Polarity	positive
Resolution at 200 m/z	60 000
AGC target	3×10^6
Maximum injection time	110 ms
Scan range	350 to 1500 m/z
DDA and MS2 settings	
TopN	15
Precursor charge states excluded from fragmentation	1, 6-8, >8
Intensity threshold	1×10^5
Isolation window	1.8 m/z
Isolation offset	0.3 m/z
Normalized collision energy for HCD	27
Resolution at 200 m/z	15 000
AGC target	2×10^5
Maximum injection time	50 ms, 75 ms [a]
Exclusion isotopes	On
Dynamic exclusion time	15.0 s, 30.0 s, 60.0 s, 120.0 s [b]
Chromatographic peak width	4 s, 7.5 s, 15 s, 30 s [c]
Apex trigger	-
Fragmentation of charge states	Single charge state, the most intense
4.2.5. Test Application 2: Multi-Attribute LC-MS Method for Characterization of Therapeutic Proteins	
MS1 settings	
Polarity	positive
Resolution at 200 m/z	60 000
AGC target	1×10^6

Table S2: Parameters of MS1 filtering, DDA, and MS/MS acquisition. (*Continued*)

Maximum injection time	118 ms
Scan range	250 to 1500 m/z
DDA and MS2 settings	
TopN	3
Precursor charge states excluded from fragmentation	1, 6-8, >8
Intensity threshold	2.5×10^5
Isolation window	2.5 m/z
Isolation offset	0.3 m/z
Normalized collision energy for HCD	27
Resolution at 200 m/z	30 000
AGC target	2×10^5
Maximum injection time	100 ms
Exclusion isotopes	On
Dynamic exclusion time	3.0 s
Chromatographic peak width	3 s
Apex trigger	1 to 3 s
Fragmentation of charge states	Single charge state, the most intense

[a)] Maximum injection time of 75 ms was set for 240-min analyses to enhance method sensitivity.

[b)] Exclusion time in seconds was calculated as gradient time in minutes divided by two.

[c)] Chromatographic peak width was increased accordingly to the expected peak broadening due to gradient extension. Individual values correspond to the used 4 gradient times in the ascending order.

Scheme S1: Common *in vitro* peptide modifications. Mass shifts are shown in brackets.

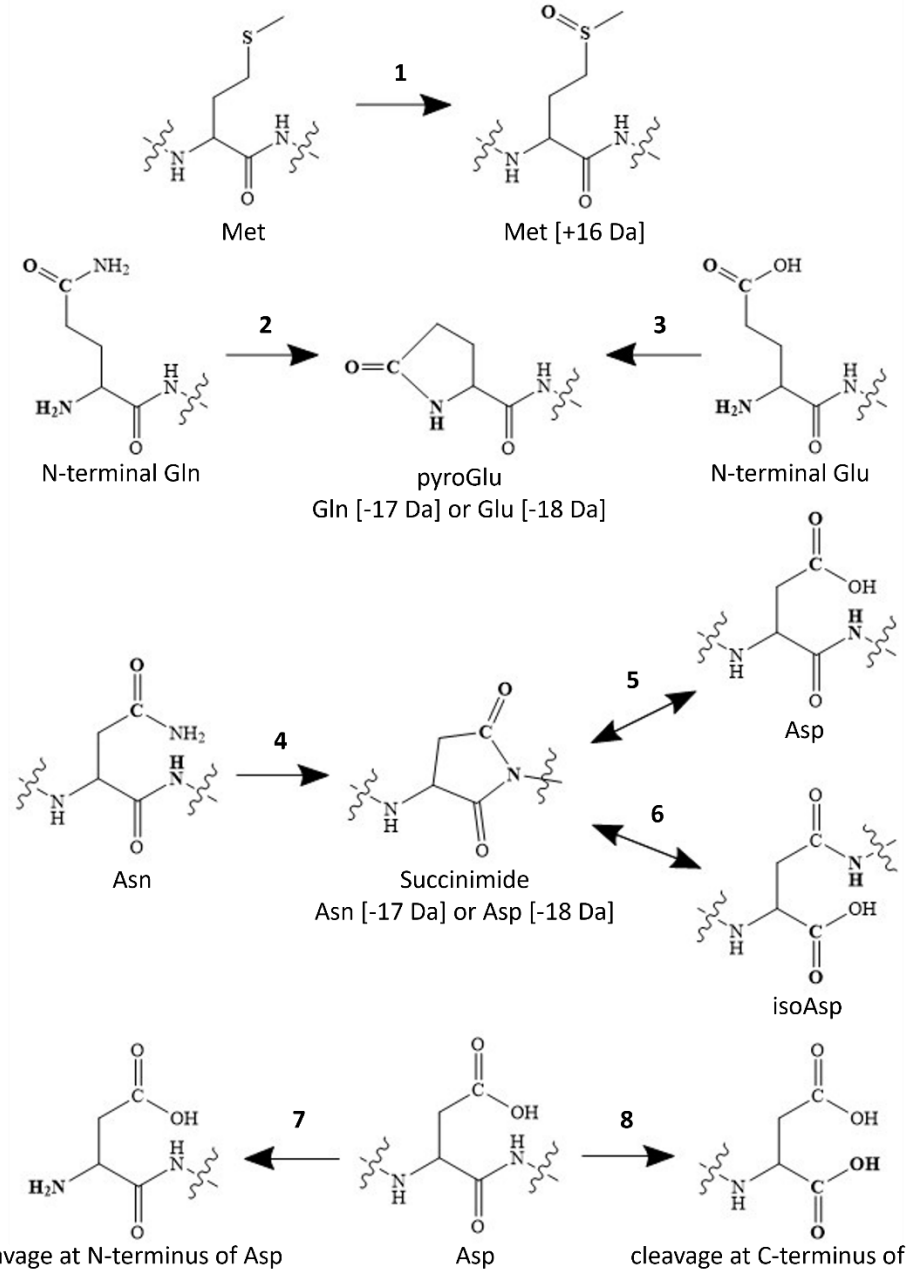

1 – Met oxidation, **2** – pyroGlu formation from N-terminal Gln, **3** – pyroGlu formation from N-terminal Glu, **4** – ammonia loss from Asn, **5** – succinimide formation from Asp (Asp dehydration), **6** – isoAsp formation from succinimide, **7** – cleavage at N-terminus of Asp, **8** – cleavage at C-terminus of Asp. Reaction **4** followed by reaction **5** or **6** in the direction of Asp/isoAsp represents the complete Asn deamidation pathway.

Figure S1: Configurations of the LC-UV (**A** and **B**) and LC-MS (**C** and **D**) instruments with/without a trap column.

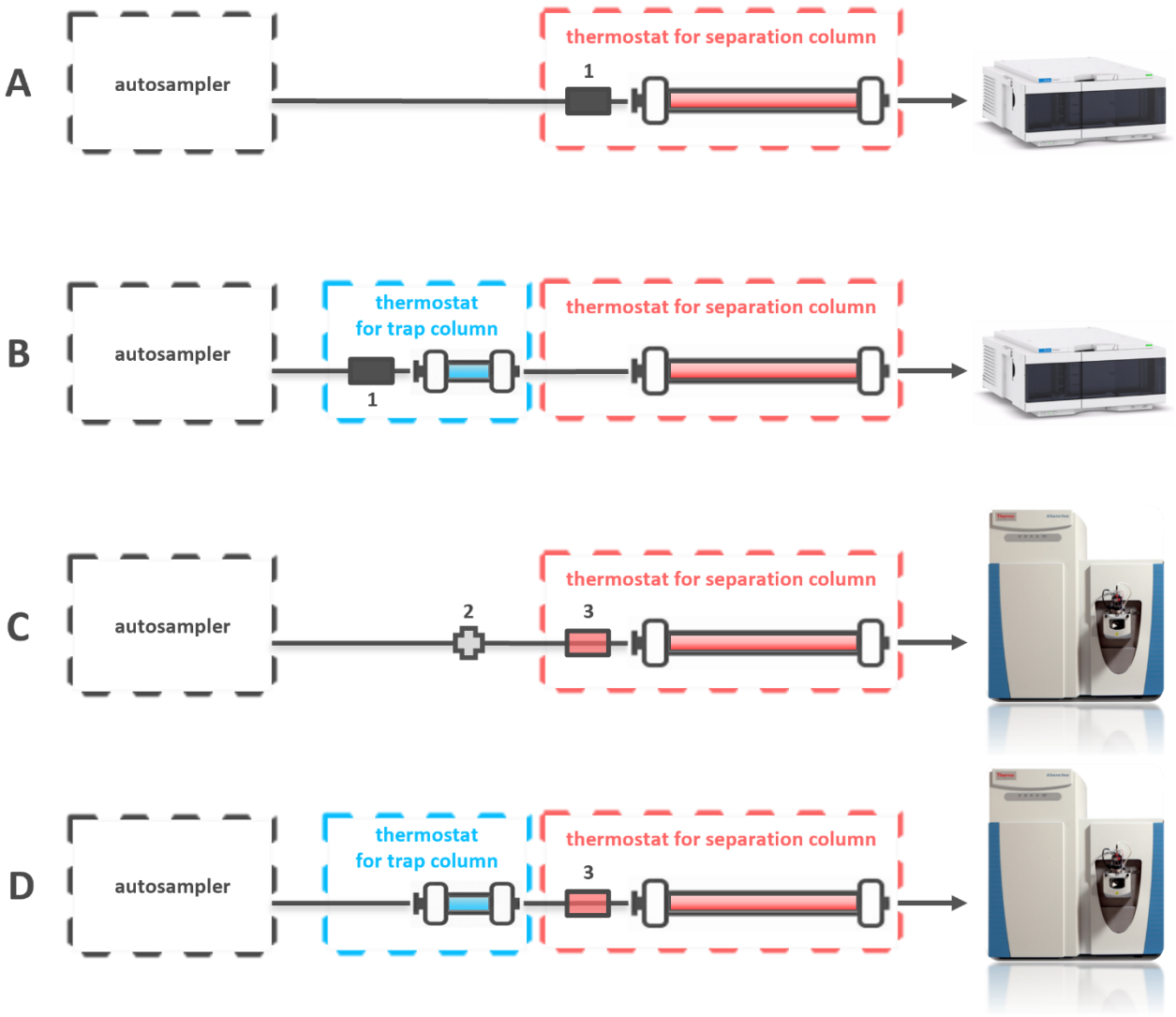

1 – Steel block of the passive preheater accommodating a major part of the whole capillary.
2 – Viper union connecting the two inlet capillaries upstream of the separation column.
3 – Active preheater assembled on the steel 0.1 × 380 mm capillary.

Figure S2: (A) Retention time and **(B)** retention factors of small-molecule analytes obtained from 4 examined trap columns of 2.1 mm i.d under the conditions of isocratic elution at 30% component B (22 °C). **(C)** Average peak widths of iRT peptides obtained using direct injection on the 2.1 mm i.d. separation column (70 °C) and the trap-elute setups including 4 trap columns (22/70 °C). The data from the 30-min gradient separation are shown. **(D)** A portion of the total in-column residence time that iRT peptides spend in trap columns of 2.1 mm i.d when it is included in the setup. Data from the 30-min separation are shown.

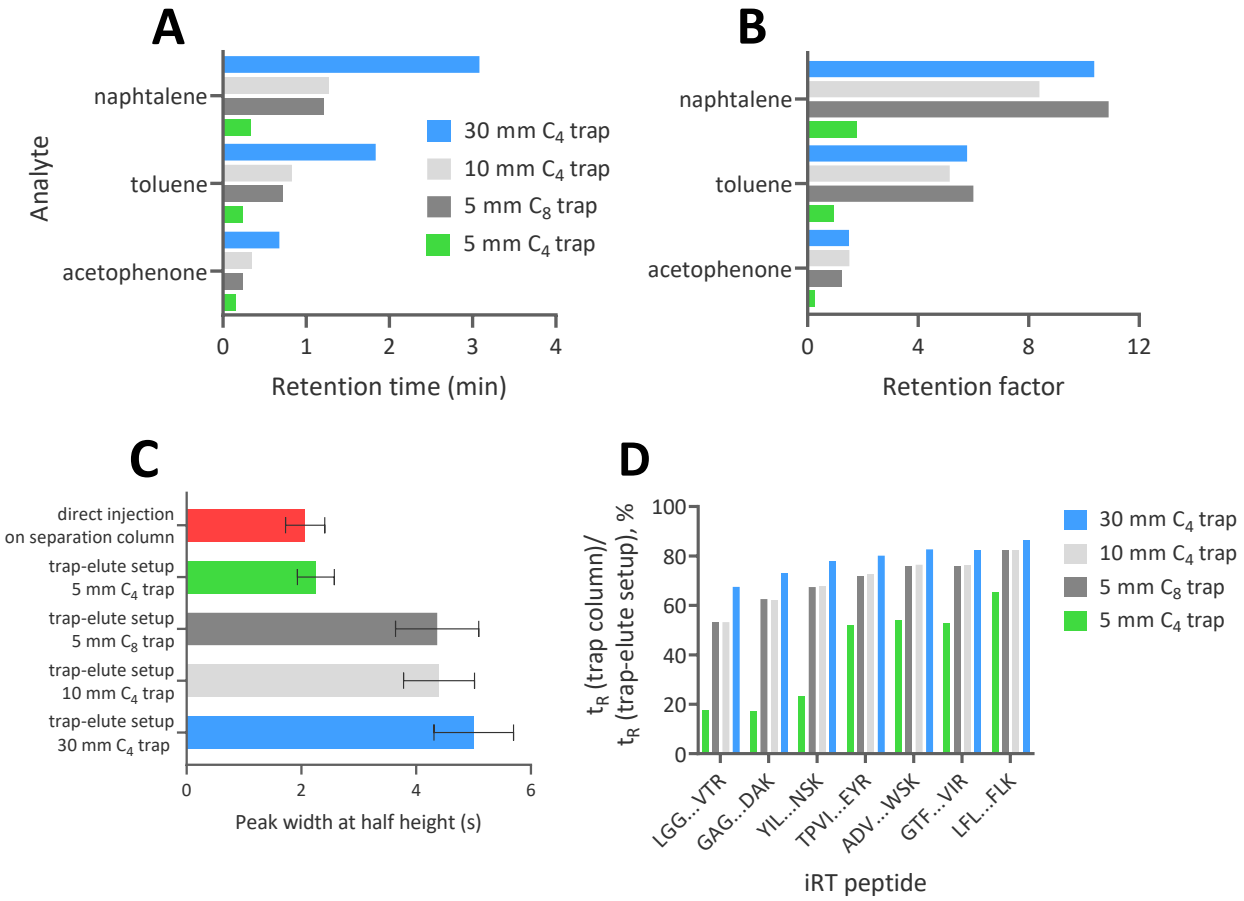

Figure S3: Average peak width of iRT peptides at half height obtained from the separation using setups of both column i.d. using mobile phase acidified with 0.05% and 0.1% formic acid.

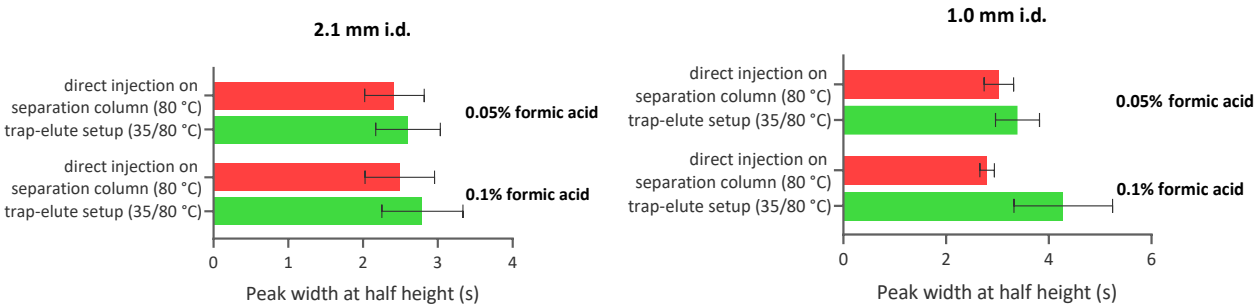

Figure S4: Extracted ion chromatogram of a peptide EVQLVESGGGL (amino acids n. 1-11 in the heavy chain of bevacizumab) with pyroGlu formed from the N-terminal Glu, which belongs to CQAs. The percentages above show the artifact peak area normalized to the peak area of intact peptide extracted from the analysis using direct injection on the heated 2.1 mm i.d. separation column. The right figure illustrates the average peak width of the given intact peptide EVQLVESGGGL under the three experimental conditions.

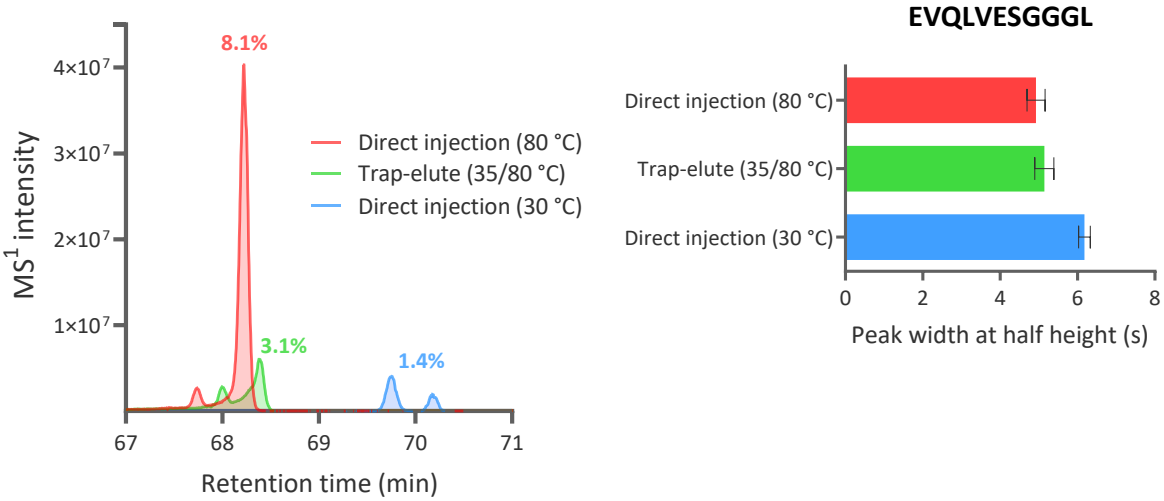

Figure S5: Extracted ion chromatograms of an intact and modified form of QTNTIIDVVLSPSHGIELSVGEK peptide (amino acids n. 97-119 in aflibercept) with pyroGlu formed from the N-terminal Gln measured using the 2.1 mm i.d. trap-elute setup and the direct injection on the 2.1 mm i.d. separation column maintained at 30 and 80 °C.